REVIEWS OF TOPICAL PROBLEMS

Spintronics: manganite-based magnetic tunnel structures

Physics – Uspekhi **55** (3) 250 – 269 (2012)

REVIEWS OF TOPICAL PROBLEMS PACS numbers: **72.25. – b**, **75.76. + j**, **85.75. – d**

Spintronics: manganite-based magnetic tunnel structures

N V Volkov

DOI: 10.3367/UFNe.0182.201203b.0263

Contents

Abstract. A topical and highly promising aspect of the field of spintronics is the physics involved in the flow of a spin-polarized current through magnetic tunnel structures. This review focuses on manganite-based structures, which are appealing for their high Curie temperature, highly spin-polarized conduction electrons, high chemical stability, and well-developed fabrication technology. Particular emphasis is placed on some novel approaches to studying the tunnel structures, including the use of planar geometry and the application of combined external factors (microwave and optical radiation) to investigate spin-polarized transport.

N V Volkov Kirensky Institute of Physics,
Siberian Branch, Russian Academy of Sciences,
Akademgorodok 50, str. 38, 660036 Krasnoyarsk, Russian Federation
Tel. + 7 (391) 243 26 35
Fax + 7 (391) 243 89 23
E-mail: volk@iph.krasn.ru

Received 21 May 2011, revised 30 August 2011
Uspekhi Fizicheskikh Nauk **182** (3) 263 – 285 (2012)
DOI: 10.3367/UFNr.0182.201203b.0263
Translated by M N Sapozhnikov; edited by A M Semikhatov

1. Introduction

Recent studies have shown that the spin degrees of freedom of charge carriers are manifested most spectacularly, and sometimes unexpectedly, mainly in magnetic and hybrid nanostructures. Investigations of the response of such systems to the flow of a spin-polarized current have brought many interesting scientific results and surprises, which have made attractive the idea of using electron spin as an active element for data storage, processing, and transfer [1, 2]. Moreover, a new, independent field in condensed matter physics was born: so-called spintronics, representing a multidisciplinary field of science and technology devoted mainly to investigations of spin-dependent electron transport in solids and low-dimensional structures. This field also involves interesting fundamental questions of spin-dependent phenomena and applied problems related to the development of novel electronic devices based on controlling spin degrees of freedom.

It is evident that the field of spintronics is quite broad, but there are strong grounds to say that two unique phenomena are currently attracting most of the attention of researchers. The first is the magnetoresistive effect in multilayer magnetic structures [giant magnetoresistance (GMR) in spin gate structures or tunnel magnetoresistance (TMR) in tunnel magnetic structures] and the second is the appearance of a

torque acting from a spin current on local magnetic moments in nanostructures (spin-transfer torque effect) [3]. In the first case, a magnetic field is used to control the magnetic state of a multilayer nanostructure, thereby providing the control of a polarized current through it. In the second case, the magnetic state of a nanostructure can be controlled with the help of a spin-polarized transport current. Moreover, the spin-transfer effect can cause magnetization precession in a ferromagnetic nanostructure at microwave frequencies [4]. Such a precession leads to the emission of microwaves at frequencies that can be controlled by both the current and the magnetic field. In fact, we are dealing with the possibility of developing microwave generators based on absolutely new principles.

The spin-transfer mechanism is also responsible for the reverse effect of the generation of a constant voltage across a magnetic tunnel junction upon irradiation by microwaves [5]. Again, we are dealing with a novel mechanism (in this case, the detection mechanism) based on the relation between the spin dynamics and polarized current in magnetic nanostructures.

Various spin-dependent effects can be observed in full measure in magnetic tunnel structures. It is no accident that studies of tunnel magnetoresistances and magnetic tunnel contacts as a whole have become an important stage in the development of spintronics and that interest in spin-polarized transport through tunnel structures only continues to grow. This review is devoted to physical processes occurring during the flow of a current through magnetic tunnel structures. We here consider only manganite-based structures. Why just manganites? We hope that our review answers this question. In brief, the reasons for this choice are as follows. First, this is the high spin polarization of conduction electrons in the chosen manganite family. Second, manganites have a comparatively high temperature of transition to the ferromagnetic state. And finally, the fabrication technology of thin manganite films, in multilayer structures in particular, is well developed. Based on experimental and theoretical studies, we analyze and estimate the advantages and disadvantages of using manganites in tunnel structures for solving various problems in spintronics.

This review is also an attempt to answer the question of whether there are real prospects for the development of spintronic devices based on manganites, which have long been considered as materials promising in many aspects for various applications. We do not aim to present a comprehensive description of all the relevant data currently available. Of course, we consider typical examples of operating manganite-based magnetic tunnel structures, but our main task is to discuss the specific features of fabrication of such structures and the flow of a spin-polarized current in them. We focus more closely on some phenomena that, in our opinion, offer quite promising applications but have been undeservedly scarcely studied so far. These include, first and foremost, the response of magnetic tunnel structures to microwave and optical radiation, the properties of structures with a current flowing in their plane (along layer boundaries), and the properties of cooperative systems of magnetic tunnel contacts.

2. Manganite-based magnetic tunnel junctions

2.1 Tunnel junction; conduction of a magnetic tunnel junction; tunnel magnetoresistance; the Julliere model

What is a tunnel junction? In the simplest case, it is a contact of two electrodes made of a conducting material, which are separated by a thin layer (~ 1 nm thick) made of an insulator or a wide-gap semiconductor. If a bias voltage is applied across the electrodes of this junction, a current flows through it, the current intensity being determined by the electron structure of the electrodes and the characteristics of the potential barrier formed by the dielectric layer. The tunnel current can be calculated using models of varying complexity.

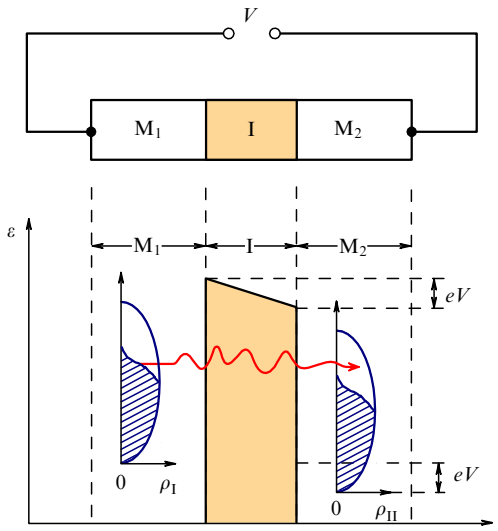

Figure 1. Scheme of the energy diagram of a normal-metal–dielectric–normal-metal junction.

We consider one of the simplest models, which nevertheless qualitatively reflects the physics of the phenomenon. Figure 1 schematically shows the energy structure of a tunnel junction. The electric voltage V applied across the junction reduces the electron energy ε in electrode M_2 by eV (e is the electron charge) compared to that in electrode M_1. The number of electrons with energy ε tunneling through the barrier from M_1 to M_2 is determined by the tunneling probability $D(\varepsilon)$, the number of occupied electron states in electrode M_1, and the number of unoccupied states in electrode M_2 with energy ε. The electric current I_1 through the structure from M_1 to M_2 is determined by the total amount of tunneling electrons with all possible energies. Because the probability of electron tunneling through the potential barrier from M_2 to M_1 is finite, the tunnel current I_2 flows in that direction. The resulting current through the tunnel structure is

$$I = I_1 - I_2 \sim \int_{\text{band}} D(\varepsilon)\left[\rho_{\text{I}}(\varepsilon)\,\rho_{\text{II}}(\varepsilon + eV) \times \left(f(\varepsilon) - f(\varepsilon + eV)\right)\right] \mathrm{d}\varepsilon\,. \quad (1)$$

The integral is taken here over the entire conduction band in a metal, $\rho_{\text{I}}(\varepsilon)$ and $\rho_{\text{II}}(\varepsilon)$ are the densities of electron states in electrodes M_1 and M_2, and $f(\varepsilon)$ is the Fermi–Dirac function. Using this approach, Simmons [6–8] obtained expressions for the tunnel current that have been most often used to date to analyze the current–voltage characteristics of tunnel structures. We note, however, that other authors have also developed similar approaches and obtained similar expressions [9–11]. The results obtained by Simmons are appealing because they were obtained in analytic form and are quite accurate, despite the approximations used.

What would change, in principle, if the electrodes in a tunnel structure were ferromagnetic? The conduction of a

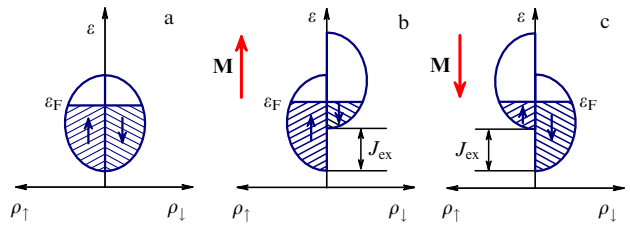

Figure 2. Band structure of normal and ferromagnetic metals: (a) normal metal; (b) ferromagnetic metal; (c) change of the magnetization direction causes a change in the splitting of the state density to the opposite one.

magnetic tunnel structure turns out to be dependent on the mutual orientation of the magnetizations of ferromagnetic electrodes. The conduction is different for parallel and antiparallel orientations of magnetizations. The reason is that the current in the ferromagnet is spin-polarized, i.e., the numbers of charge carriers with different spin projections in the ferromagnet are different. In this case, it is necessary to account for the additional degree of freedom of conduction electrons in magnetic nanostructures, their spin state, and consider spin-dependent effects manifested in the different behavior of electrons with opposite spin projections, which we call spin 'up' (↑) and spin 'down' (↓) in what follows (or 'majority spin' and 'minority spin', respectively). The spin polarization in metals, which have spontaneous magnetization, appears naturally due to the spin splitting. The exchange interaction causes a relative shift of the energy subbands for electrons with spins up and down by the exchange energy J_{ex} (Fig. 2). Due to the asymmetry produced in the electron state density, the numbers of electrons with different spin projections near the Fermi level (ε_F) become different, i.e., a spin polarization appears in the magnetic material. The polarization is usually defined as

$$P = \frac{\rho_\uparrow(\varepsilon_F) - \rho_\downarrow(\varepsilon_F)}{\rho_\uparrow(\varepsilon_F) + \rho_\downarrow(\varepsilon_F)}\,. \tag{2}$$

We explain the key role of spin polarization for the conduction of a magnetic tunnel structure with the example of the simplest Julliere model, which has already become classic [12]. This model describes the conduction of a magnetic tunnel transition using two simple assumptions: (i) The electron spin is preserved during tunneling through the barrier and (ii) (a direct consequence of the first assumption) the tunneling current can be divided into two channels with spins up and down. These assumptions are based on previous studies of the spin polarization of electrons in ferromagnetic metals and spin-polarized tunneling between a ferromagnet and a superconductor. Electrons with spin up in one electrode tunnel only to the subband of electrons with spin up in the other electrode, and vice versa. A simple band structure illustrating this is shown in Fig. 3.

According to Julliere's assumption, the currents for parallel (P) and antiparallel (AP) configurations can be written as the sums of currents in two 'spin' channels:

$$I_P = I_P^\downarrow + I_P^\uparrow\,, \tag{3}$$

$$I_{AP} = I_{AP}^\downarrow + I_{AP}^\uparrow\,. \tag{4}$$

For the parallel configuration of the magnetic moments of electrodes, $\mathbf{M}_1 \uparrow\uparrow \mathbf{M}_2$, the current through the magnetic

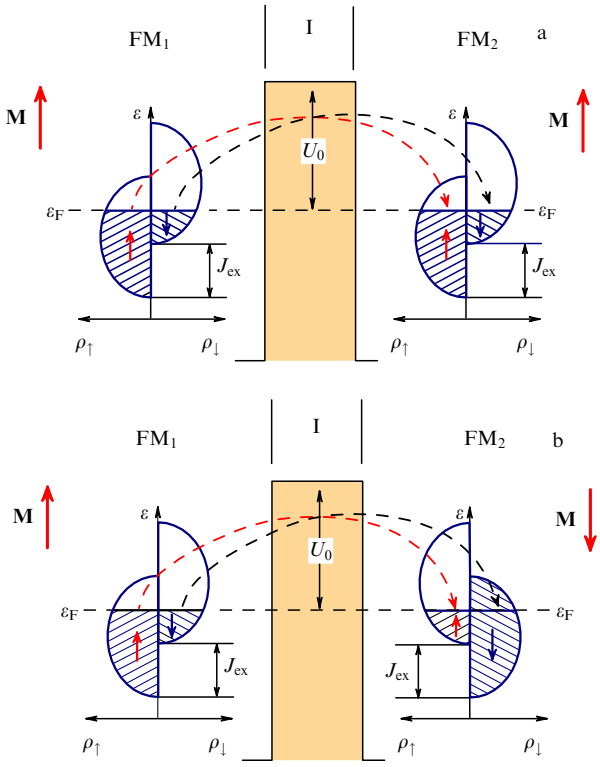

Figure 3. Schematic representation of electron tunneling between two ferromagnetic electrodes FM_1 and FM_2: (a) magnetizations of both electrodes are parallel; (b) magnetizations are antiparallel.

tunnel junction at $T = 0$ K is

$$I_P \propto D(\varepsilon_F)\left[\rho_1^\uparrow(\varepsilon_F)\,\rho_2^\uparrow(\varepsilon_F + eV) + \rho_1^\downarrow(\varepsilon_F)\,\rho_2^\downarrow(\varepsilon_F + eV)\right], \tag{5}$$

where $\rho_{1,2}^\uparrow$ and $\rho_{1,2}^\downarrow$ are the densities of states for electrons with spins up and down in the first and second electrodes. In the antiparallel configuration, $\mathbf{M}_1 \uparrow\downarrow \mathbf{M}_2$, after the reversal of the direction of $\mathbf{M}_2$, the tunnel current in the ferromagnetic contact is given by

$$I_{AP} \propto D(\varepsilon_F)\left[\rho_1^\uparrow(\varepsilon_F)\,\rho_2^\downarrow(\varepsilon_F + eV) + \rho_1^\downarrow(\varepsilon_F)\,\rho_2^\uparrow(\varepsilon_F + eV)\right] \tag{6}$$

because, under the reversal of $\mathbf{M}_2$, the state densities for electrons with spins up and down are also reversed. Julliere defined the relative change in the tunnel resistance caused by the change in the mutual orientation of the magnetization of electrodes, which was called the tunnel magnetoresistance (TMR), as

$$\mathrm{TMR} = \frac{I_P - I_{AP}}{I_{AP}} = \frac{R_{AP} - R_P}{R_P}\,. \tag{7}$$

When a voltage applied across the tunnel junction is low ($V \sim 0$), the TMR is described, taking (2) into account, by the simple expression

$$\mathrm{TMR} = \frac{2P_1P_2}{1 - P_1P_2}\,, \tag{8}$$

where P_1 and P_2 are spin polarizations for the first and second electrodes of the structure. Of course, this model cannot

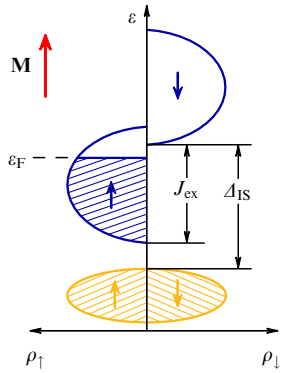

Figure 4. Band structure of a semimetal. Δ_{IS} is the dielectric gap for electrons with spin down.

explain the temperature dependence of the TMR, the dependence on the bias voltage, and many other properties. However, numerous experiments show that despite its simplicity, the Julliere model predicts the TMR value in high-quality tunnel contacts of two ferromagnetic electrodes for $V \sim 0$ quite accurately.

It becomes clear, even from the simple example considered above, that a key problem that should be solved to fabricate efficiently 'operating' magnetic tunnel transitions both for studying fundamental issues and for applications in spintronic devices is to provide the highest possible spin polarization in electrodes forming a tunnel junction. The search for materials with a high spin polarization has therefore come to the fore. On the one hand, ferromagnetic 3d metals and their alloys are attractive because thin films of these materials can be comparatively simply fabricated, and these metals have a high temperatures T_C of transition to the ferromagnetically ordered state. However, calculations and experimental studies indicate that maximal polarizations for ferromagnetic transition metals do not exceed 10–45%. At the same time, other classes of ferromagnetic materials exist, so-called 'half-metal ferromagnets', which have the metallic conduction for one spin direction and dielectric properties for the other spin direction (Fig. 4). In other words, these materials have the 100% spin polarization. They also include manganites of a certain composition, which makes them promising materials for use in magnetic tunnel structures and elements of spintronic devices.

2.2 Manganites: Basic properties

Manganites are a class of materials with the structural formula $M_xA_{1-x}MnO_3$ (M = La, Pr, Nd, Eu..., A = Ca, Sr, Pb...) and a perovskite-like structure. These materials can be justifiably called unique. The presence of strongly interacting spin, charge, and orbital subsystems determines their rich (x, H, T) phase diagram [13]. Depending on the composition (x), temperature (T), external magnetic field (H), and other external perturbations, manganites can be in metallic and dielectric ferromagnetic states, the antiferromagnetic state, and states with charge and orbital ordering.

For certain doping levels, the interaction energies responsible for the formation of one phase or another become comparable and the question of the ground state of the system becomes rather subtle. It is assumed that the ground state can then be an inhomogeneous state with phase separation. This state is in thermodynamic equilibrium and is not caused by the trivial chemical inhomogeneity of the materials under study. The reason is the competition of interactions of comparable strengths in the system. A delicate energy balance leads to a high sensitivity of systems with phase separation to the external actions of temperature, magnetic field, pressure, transport current, and optical radiation.

The action of the magnetic field on a phase-separated state most likely leads to the colossal magnetoresistance (CMR) effect and many other quite interesting effects. These include a current-induced change in the magnetic state [14], a current-induced metastable resistive state [15], a nonlinear electric response [16], giant non-Gaussian resistance fluctuations [17], an optically induced conduction response [18], and a change in the type of transition to the ferromagnetic state [19]. Although many properties, including the unique CMR effect, are still not fully understood, they are considered to be promising for practical applications, in particular, in spintronic devices.

In concluding this section, we note that different aspects of the physics of manganites mentioned above are discussed in excellent reviews and books [13, 20–23]. Our review is mainly devoted to issues concerning the features of the electron structure on the surface (near interfaces with other materials) of ferromagnetic manganites with metallic conduction and also the efficiency of using these materials as injectors and detectors of polarized electrons in nanostructures.

2.3 Manganites as materials with a high spin polarization

Manganites have also attracted great interest due to their properties not related to phase separation. It was found that some manganese oxides with a perovskite structure can belong to the class of half-metal ferromagnets, i.e., materials in which only one spin subband is occupied at the Fermi level, resulting in a 100% spin polarization. Because the spin polarization value plays a key role in the manifestation of spin-dependent effects, manganites have been extensively studied as promising sources and detectors of polarized electrons in magnetic low-dimensional structures. 'Classic' manganites with compositions close to $La_{2/3}Sr_{1/3}MnO_3$ and $La_{2/3}Ca_{1/3}MnO_3$ (below, we let LCMO denote Sr-doped manganites by LSMO and La–Ca manganites) have been studied most often. These materials have metallic conduction below the ferromagnetic-state transition temperature and rather high T_C values. The so-called 'optimally doped' manganites $La_{2/3}Sr_{1/3}MnO_3$ and $La_{2/3}Ca_{1/3}MnO_3$ respectively have $T_C \approx 370$ K (the highest T_C among manganites) and ≈ 270 K. The metallic conduction, high ferromagnetic-state transition temperatures, high chemical stability, and well-developed fabrication technology of these manganites make them very attractive objects of investigation.

Despite predictions made in the mid-1990s that LSMOs and LCMOs belong to the class of half-metal ferromagnets [24], numerous experimental data on the spin polarization of these materials obtained by different methods proved to be rather contradictory. One of the most powerful and well-developed methods for measuring the spin polarization of electrons in ferromagnets is the method of superconducting tunnel spectroscopy [25]. It is based on the measurement of the conduction of a tunnel ferromagnet–insulator–superconductor contact and analysis of the results using the dependence of the state density of quasiparticles in a superconductor on the tunnel current and the notion of spin splitting of the superconducting state density in a magnetic

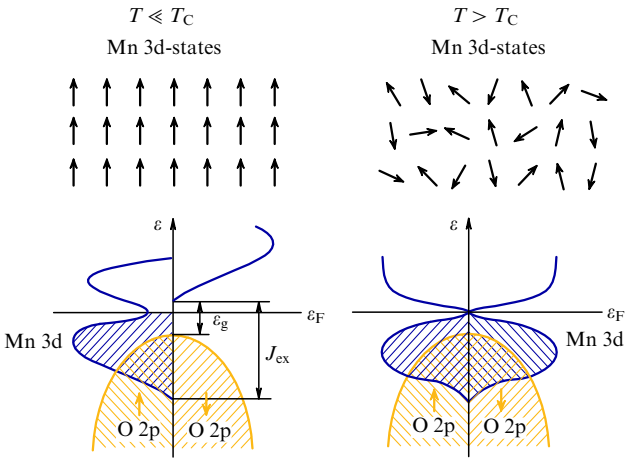

Figure 5. Energy level diagram for manganite at $T \ll T_C$ and $T > T_C$. J_{ex} is the exchange energy and ε_g is the dielectric gap in the density of states for electrons with spins directed oppositely to the magnetization direction [27].

field. However, measurements of the tunnel conduction in high-quality contacts with $SrTiO_3$ (STO) and LSMO/STO/Al barriers [26] gave the spontaneous polarization for manganite as only 72%. The authors assumed that the value of P could be affected by the manganite–barrier interface.

Another method for studying spin polarization is spin-resolved photoemission spectroscopy. The authors of [27] studied LSMOs by this method and concluded that below T_C, this manganite belongs to half-metal ferromagnets. The results of these studies are presented schematically in Fig. 5. For $T \ll T_C$, the spins of 3d electrons of Mn are oriented as in ferromagnets due to the double-exchange ferromagnetic interaction. Hence, the 3d states of manganese ions, which extend up to ε_F, have only one spin state (spin up).

The 2p states of oxygen, which have both directions of spin (the density of states is symmetric for electrons with spins up and down), are located 0.6 eV below the Fermi energy. Therefore, the metallic conduction is determined by charge carriers in the 3d states of Mn ions with only one spin direction (spin up). For the other, 'minority spin' direction (spin down), the unfilled 3d states of Mn are separated by a dielectric gap from the filled 2p states of oxygen.

At temperatures above T_C, the spin polarization of charge carriers disappears. Indeed, magnetic moments of manganese ions become disordered and the asymmetry in the 3d density of states of Mn for two spin directions disappears. Due to the double-exchange interaction, the loss of the ferromagnetic order in the system reduces the electron transfer energy, and the electron state density at ε_F almost vanishes.

2.4 Manganite-based magnetic tunnel junctions

The high spin polarization of charge carriers in manganites can be confirmed by direct studies of magnetic tunnel junctions with manganite electrodes and the TMR value in them. The first experiments with tunnel LSMO/STO/LSMO contacts have already demonstrated the very large TMR at low temperatures corresponding to the spin polarization $P > 0.8$ [28–30]. At the same time, this high spin polarization rapidly decreases with increasing the temperature and virtually vanishes at about 250 K, which is much lower than the ferromagnetic ordering temperature in LSMO (370 K). This behavior can be explained in two ways [31]. It can be related either to an intrinsic surface effect in manganites, namely, to the reduction of the exchange interaction in the surface region, or to the quality of the manganite–dielectric interface, which is produced at the technological stage and depends on the material of the potential barrier. In fact, both these reasons affect the spin polarization value.

It has now become clear that the degree of polarization is mainly determined not by the properties of a bulk ferromagnet but by the properties of the material surface near the interface (or even of the ferromagnetic metal–insulator interface a few atomic layers in width [1, 32]). Manganites have their specific features. These materials are extremely sensitive to local crystal properties, and therefore the defect surface structure of manganite and surface structural stresses induced by the difference in the lattice constants of manganite and barrier material can considerably suppress the ferromagnetic order in surface layers. Moreover, the ferromagnetic order suppression can be accompanied by a suppression of the conducting properties of the surface layer, which inevitably affects the conservation of the spin polarization of the current flowing through this layer. It seems that just the loss of magnetic properties in the interface layer can explain the disappearance of spin polarization in bulk manganite at temperatures considerably lower than T_C, irrespective of the potential barrier nature.

Of course, the quality of the manganite–barrier interface and therefore the polarization of tunneling electrons also depend on the barrier material. Tunnel junctions with $SrTiO_3$, $Ce_{1-x}La_xO_{2-x/2}$, $PrBaCu_{2.8}Ga_{0.2}O_7$, and $NdGaO_3$ barriers studied in [33] confirmed the conclusions made above. The best result among manganite-based magnetic tunnel junctions was probably obtained for the all-epitaxial three-layer LSMO (35 nm)/STO (2.8 nm)/LSMO (10 nm) structure [34]. The structure was prepared by pulsed laser deposition. The authors paid special attention to the quality of the LSMO/STO boundaries. Scanning electron energy loss spectroscopy performed at atomic resolution revealed that the electronic properties of LSMO were only slightly modified at the interface with the STO barrier, compared to regions inside the LSMO layer. The tunnel junction was prepared by the methods of UV lithography and ion etching. The size of tunnel junctions did not exceed 6×6 mm. The magnetoresistance of these junctions reached 1800% at 4 K (Fig. 6). In the framework of the Julliere model, this corresponds to the

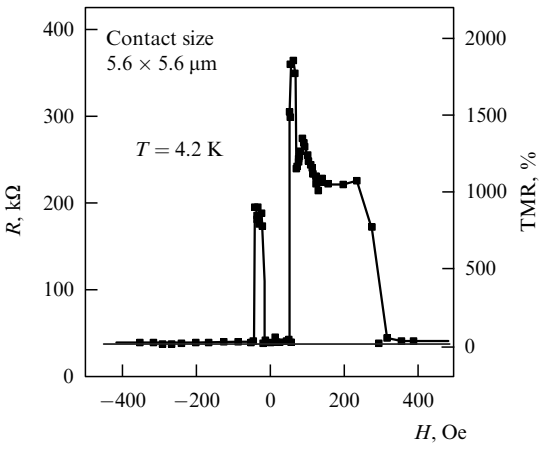

Figure 6. Dependence of the tunnel magnetoresistance of an $La_{0.7}Sr_{0.3}MnO_3SrTiO_3/La_{0.7}Sr_{0.3}MnO_3$ magnetic tunnel contact on the magnetic field [34].

spin polarization of manganite electrodes not less than $P \sim 95\%$. This result confirms once more that LSMO manganite can be assigned to the class of half-metallic ferromagnets and can be used, in principle, by employing well-developed technology in elements of spintronic devices. At the same time, the magnetoresistive effect and hence the nonzero spin polarization was preserved in the case under study only up to 270 K. Although this temperature is higher than that observed in other experiments, we cannot yet speak about prospects of wide practical applications of manganites.

It is also necessary to discuss a number of aspects concerning the choice of materials for tunnel barriers (incidentally, this concerns not only manganite-based tunnel junctions) [35]. The main requirement for an insulating layer between ferromagnetic electrodes to play the role of a potential barrier is the homogeneity and the absence of defects and impurities in the insulator. On the one hand, the trivial scattering of electrons by defects (especially paramagnetic defects) results in the loss of their 'spin memory' during tunneling. On the other hand, in the presence of defects of a certain type, transport in a barrier can occur in the charge carrier hopping mode with a variable hopping distance, when electrons tunnel between successive defect states, finally resulting in the loss of the spin-polarized electronic state after the propagation of electrons through the potential barrier.

The tunnel current in magnetic tunnel junctions strongly depends on the electron structure near the interfaces between ferromagnetic electrodes and the insulating barrier. Indeed, as we mentioned above, numerous experiments and calculations show that the TMR value and behavior are determined only by a few monolayers of electrode materials near the ferromagnetic–insulator interface. This can be simply explained by the penetration of atoms from the electrode into the barrier, and vice versa near the interface, caused by the fabrication technology, which leads to the appearance of impurities or the formation of a nonstoichiometric composition. As a result, the spin-polarized state of charge carriers is lost on interfaces of the structure. But even if the interface is made ideal, the formation of a chemical bond between atoms of a ferromagnetic metal and an insulator can cause drastic changes in the electron structure of the interface. The character of the chemical bond is determined only by the nature of bound materials. As a result, for example, spin polarizations in the ferromagnetic volume and at the interface with an insulator can considerably differ, up to the loss of the spin polarization or the change of its sign after the propagation of electrons through the interface. The type of the bond also determines the efficiency of propagation of electrons through the interface.

2.5 Use of manganite-based tunnel junctions for the analysis of spin information

We concluded above that the absence of spin polarization at room temperature is the main obstacle to practical applications of manganites as elements in spintronic devices. However, the high (in fact, record high) spin polarization at

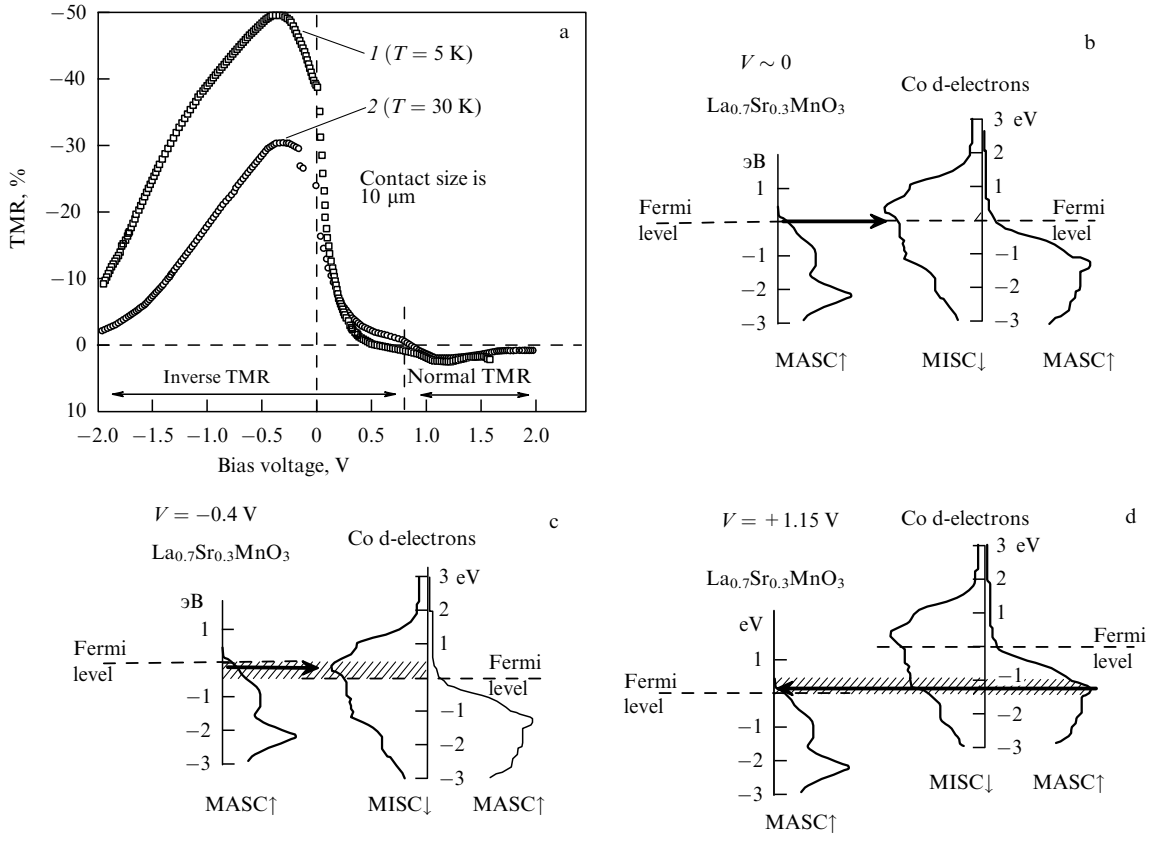

Figure 7. (a) Tunnel magnetic resistance of Co/STO/LSMO tunnel junctions 10 μm in size as a function of the bias voltage. (b–d) Relative position of the d-electron density of states in Co and $La_{0.7}Sr_{0.3}MnO_3$ for different bias voltages; the figures explain the relation between the TMR and the electron density of states in ferromagnetic electrodes having a tunnel structure; the arrows show tunneling directions; the hatched regions are those in the electron density of states for Co and $La_{0.7}Sr_{0.3}MnO_3$ whose electrons make the main contribution to the tunnel current [38].

low temperatures, the well-developed fabrication technology of high-quality thin manganite films, the reproducibility of their properties, and well-developed methods for calculating the electron structure of manganites gave a powerful impetus to the extensive use of these materials in experimental studies of spin-dependent transport properties, for studying the band structure of materials, and as efficient spin injectors and detectors.

The idea of such applications of manganites was proposed and realized already in the late 1990s, when it was found that their spin polarization approaches 100%. First of all, the study of the conduction and TMR in a structure with LSMO/STO/LSMO manganite electrodes as functions of the bias voltage gave a quite accurate quantitative description of the band structure of the manganite itself [36]. These results were in good agreement with experimental data obtained by spin-polarized inverse photoemission. The authors pointed out that magnetic tunnel structures with electrodes made of half-metallic ferromagnets are very promising for spin-resolved spectroscopic studies.

The detection of a positive magnetoresistance of the Fe_3O_4/STO/LSMO heterostructure showed that the specific feature of the electron structure of manganite is that electron states with an antiparallel spin direction with respect to the magnetization of a ferromagnet dominate at the Fermi level [37]. Ferromagnets of this type are called minority spin carrier (MISC) ferromagnets, unlike majority spin carrier (MASC) ferromagnets, in which the spins of charge carriers are aligned parallel to the total magnetization.

The use of LSMO as a spin analyzer in the tunnel Co/STO/LSMO contact and the study of TMR also provided information on the electron density of states of ferromagnetic cobalt [38]. Indeed, the behavior of TMR and a change in the value, and even sign, upon changing the bias voltage across the tunnel junction adequately reflect the structure of spin subbands in the electron density of states (Fig. 7).

We also note that tunnel structures based on hole-doped ($La_{0.7}Ca_{0.3}MnO_3$) and electron-doped ($La_{0.7}Ce_{0.3}MnO_3$) manganites were studied in [39]. The magnetoresistive characteristics of the structure showed that $La_{0.7}Ce_{0.3}MnO_3$ belongs to MISC ferromagnets and has a high degree of spin polarization. In fact, this manganite can be assigned to the class of half-metallic ferromagnets. This result is quite attractive, because the combination of hole- and electron-doped manganites can open up new possibilities in the development of spintronic devices.

We now consider in more detail a rather unusual, but quite demonstrative example of the use of manganites, namely, the study of spin-polarized transport in a nonmagnetic carbon nanotube (CNT) [40]. The authors investigated the specific features of spin transport in nanotubes. Such experiments have become very popular in recent years because of the long lifetime of spin states in nanotubes due to a weak spin–orbit interaction and to the high Fermi velocity of charge carriers. It is remarkable that a measurement device contains epitaxial LSMO electrodes operating as a source and a drain of polarized electrons. The electrodes are fabricated to provide a sharp and independent switching of the magnetization between parallel and antiparallel configurations, while the electric contact between electrodes is provided by a single multiwall CNT lying above on the electrodes (Figs 8a, b). Such a geometry and, most importantly, the use of manganite electrodes immediately provided

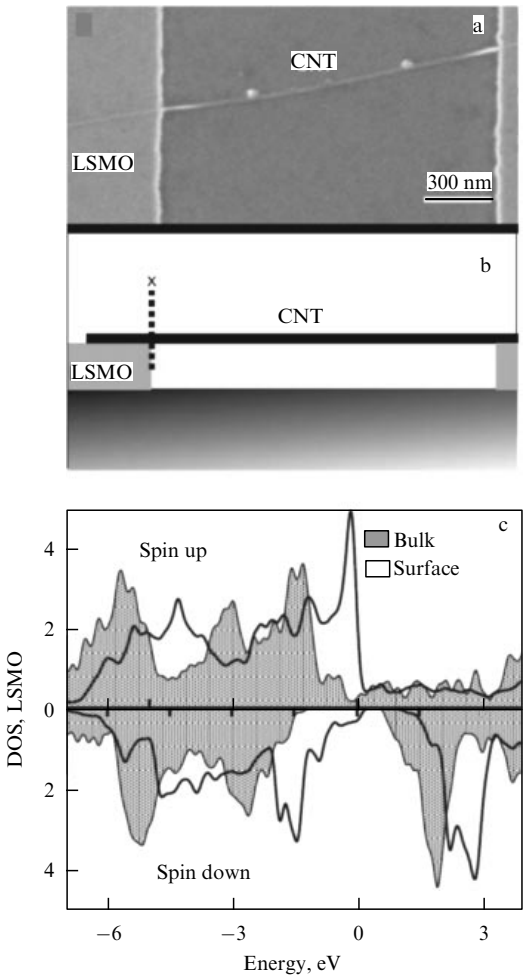

Figure 8. (a) Scanning electron microscope image of a carbon nanotube between two LSMO electrodes; (b) schematic image of the nanotube position on the electrodes; (c) *ab initio* calculations of the density of electronic states (DOS) for spins up and down in the LSMO bulk and on the surface [40].

a solution to several experimental problems. First, LSMO provides a high spin polarization of the electrodes (no less than 80%), which is maintained at the LSMO–CNT interface. This result was confirmed by *ab initio* calculations performed by the density functional method (Fig. 8c). Second, the LSMO is an oxide compound with high chemical stability and high stability with respect to external perturbations. This allows fixing nanotubes on the electrodes of a measurement device *ex situ*. Finally, the 'conduction mismatch' problem was solved in a natural way.

This rather unusual problem was first formulated in the study of the efficiency of spin injection from a ferromagnetic metal to a semiconductor [41]. The current penetrating a semiconductor in contact with a ferromagnetic metal was found to be almost completely depolarized. The solution to this problem was proposed in [42, 43]. The authors proposed performing an injection (extraction) of the spin-polarized current into a semiconductor (from a semiconductor) using a spin-dependent surface resistance. This can be realized by forming a tunnel junction at the metal–semiconductor interface. The efficiency of the injection (extraction) through a tunnel junction was experimentally demonstrated in [44]. In our example, a tunnel junction is naturally produced at the

LSMO–CNT interface, which solves the problems of the efficient injection of a spin-polarized current into a nanotube and detection of the spin states of electrons.

We note in conclusion that studies of a device containing ferromagnetic elements and a nonmagnetic current channel (CNT) have demonstrated a very large magnetoresistive effect (61% at 5 K), greatly exceeding the values obtained earlier for similar systems. This suggests that the spin relaxation time in CNTs is actually quite long, and manganites and carbon nanotubes are well matched in devices based on spin-polarized materials. The authors believe that this result is general and will be valid not only for CNTs of a certain type but also for a wide class of carbon low-dimensional systems. Therefore, carbon systems are promising for numerous applications and, in particular, can be combined with ferromagnetic manganites for the development of spintronic devices. Other investigations of spin-dependent effects in nanotubes and some organic materials, where manganites are used as efficient sources and detectors of a polarized current, are considered in review [45].

3. Spin-dependent transport properties of manganite-based tunnel structures in the 'current-in-plane' geometry

3.1 Current-driven switching of current channels; nonlinear transport properties

The effects of spin-dependent transport in magnetic tunnel structures are usually studied in the geometry where the current is perpendicular to the plane (CPP) (Fig. 9a). Of course, this is the most natural geometry in which the observed effects can be interpreted simply. At the same time, the question arises of whether the use of the current-in-plane (CIP) geometry, in which the current flows parallel to the interface (Fig. 9b), can give something new. It is well known, for example, that the giant magnetoresistance effect in multilayer gate ferromagnetic-metal–normal-metal structures is observed in both CPP and CIP geometries. The first experiments with such structures were performed by passing the electric current along structure layers [1].

Interesting effects have been observed in the CIP geometry for multilayer ferromagnetic-metal–insulator–semiconductor hybrid structures [46, 47]. Studies in the CIP geometry are also stimulated by the fact that it is possible to produce a two-dimensional electron gas in tunnel structures along the semiconductor–insulator interface, which determines the transport properties of structures in the planar geometry. We can expect new manifestations of the electron transport in magnetic tunnel structures in which the current flows along structure layers. In addition, the use of the CIP geometry is sometimes also preferable from the practical standpoint, for example, in the same hybrid semiconductor

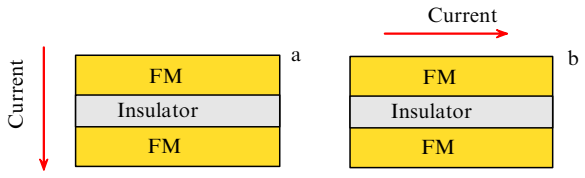

Figure 9. Two types of multilayer magnetic structures for studying transport properties: (a) CPP geometry, (b) CIP geometry.

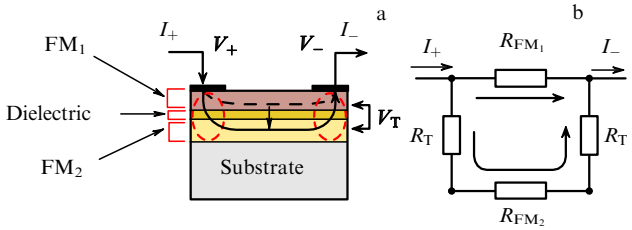

Figure 10. (a) Magnetic tunnel structure in the CIP geometry; (b) equivalent electrical circuit.

structures combining ferromagnetic elements and elements of conventional semiconductor electronics in which, as is well known, the planar technology is used.

In our opinion, this problem has not been adequately studied in the literature, and we therefore discuss it in detail. We consider the possible scenarios of electron transport in the CIP geometry in the example of a hypothetical magnetic tunnel structure consisting of two ferromagnetic conducting layers separated by a thin insulating layer (Fig. 10). Because current contacts are deposited on the upper conducting layer (FM_1), while the lower conducting layer (FM_2) is separated by the potential barrier (dielectric), it is reasonable to assume that the current would flow over the upper electrode and all transport properties would be determined by the properties of the upper film. There is nothing interesting in this. We now assume that the resistance R_{FM_1} of the upper layer considerably exceeds the resistance R_{FM_2} of the lower layer ($R_{FM_2} \ll R_{FM_1}$). For low voltages across the structure, the current, as assumed above, flows over the upper layer, but as the voltage V across the current contacts is increased, the bias voltage V_T appears across tunnel junctions between contacts. The increase in that voltage reduces the resistance R_T of tunnel junctions, and when R_T becomes smaller than the resistance R_{FM_1} of the upper film, the switching of the current channel occurs. The current begins to flow mainly over the lower layer of the structure. In this case, a drastic change in the current–voltage characteristics (CVCs) of the structure should be expected. Because the resistance of tunnel junctions depends on the mutual orientation of the magnetization of ferromagnetic layers, it is possible to use a magnetic field to control the switching of current channels in structures with the CIP geometry. Such a controllable switching must be manifested as the magnetoresistive effect.

The described scenario of the controllable switching of current channels is manifested in full measure in the $La_{0.7}Sr_{0.3}MnO_3$ manganite tunnel structure. Following the results obtained in [48–50], we demonstrate the possibility of observation of new transport and magnetotransport properties in a magnetic tunnel structure in the CIP geometry.

The tunnel structure was prepared by the method of pulsed laser-induced evaporation on a (001) SiO_2 substrate. The Si and LSMO layers were successively deposited on the substrate, and then the structure was annealed in oxygen atmosphere. As a result, the structure acquired the form shown in Fig. 10a. It consists of three layers: the 10-nm-thick manganese monosilicide (MnSi) lower layer, the LSMO film upper layer up to 100 nm in thickness, and the magnesium-deficient manganite ($LSM_{1-\delta}O$) layer up to 5 nm in thickness. Such a composition was formed due to the efficient diffusion of Mn to Si [51]. The $LSM_{1-\delta}O$ layer produced in this process proves to be an insulator playing the role of a potential barrier between MnSi and LSMO

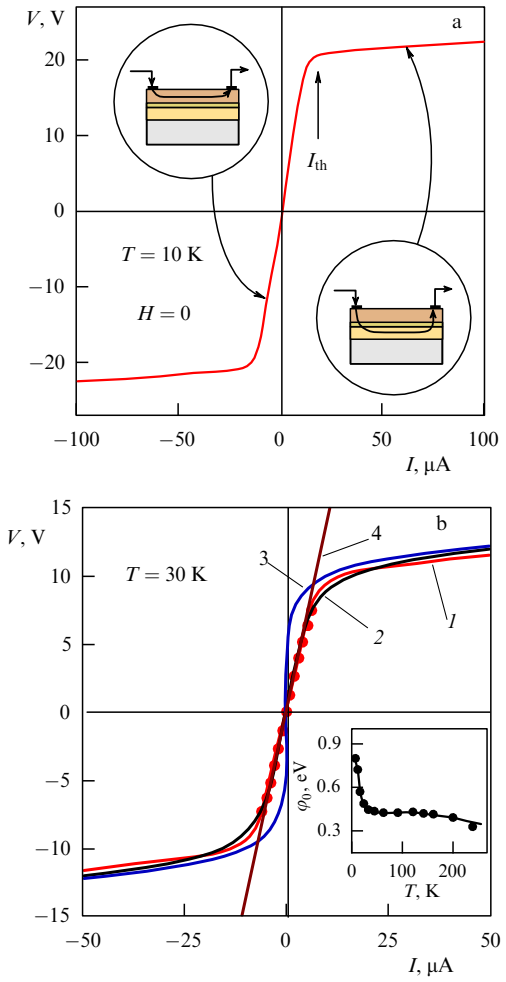

Figure 11. Magnetic tunnel structure in the CIP geometry. (a) CVC structures; insets explain qualitatively that a drastic change in the CVC behavior is caused by the switching of the current channel at the current I_{th}. (b) Approximation of the CVC by means of the equivalent circuit shown in Fig. 10b: (1) Experimental dependence, (2) approximation, (3) CVC of a tunnel junction (Simmons formula), (4) CVC of the upper LSMO film; the inset shows the temperature dependence of the mean height of the potential barrier obtained in the approximation.

electrodes. As regards the lower layer, it is known that MnSi has metallic conduction and the ferromagnetic transition temperature ~ 30 K [52], which is confirmed by magnetic measurements.

The transport properties under investigation can be conventionally divided into two parts: nonlinear transport properties and the influence of a magnetic field on structure conduction. We first consider the nonlinear properties. The CVCs of the structure have an almost linear initial part, which is followed at a critical current I_{th} by a drastic change in the CVC slope (Fig. 11a). This behavior can be explained as follows. For small values of I, we observe a linear dependence $V(I)$, as should be expected for manganites. An increase in I gives rise to a bias voltage V_T ($V_T \ll V$) across tunnel junctions between current contacts, resulting in an increase in the tunnel current I_T through the potential barrier separating the upper and lower structure layers. As a result, for $I > I_{th}$, the current begins to flow predominantly over the MnSi layer, whose resistance R_S is small compared to the resistance of R_M of the manganite film. The approximation of experimental CVCs in the framework of an equivalent circuit (Fig. 10b), involving the Simmons formula [7] obtained for the tunnel current I_T in the approximation of elastic tunneling through the potential barrier, is quite satisfactory (Fig. 11b). The values of fitting parameters were as follows: the potential barrier width was $\Delta x = 5$ nm, while the average height of the potential barrier changed with temperature from $\varphi_0 \cong 0.3$ eV at 250 K to $\varphi_0 \cong 0.8$ eV at 5 K (inset in Fig. 11b), in accordance with the structural data. The change in φ_0 can be caused by the change in the electron structure of materials used in the tunnel junction during ferromagnetic ordering [53]. Below T_C, some manganites exhibit an anomalously large shift of the chemical potential, proportional to the manganite magnetization squared. Thus, the work function of manganite increases after its transition to the ferromagnetic state, compared to the depleted boundary layer remaining in the nonmagnetic state and playing the role of a potential barrier. As a result, φ_0 increases upon increasing the manganite magnetization. This is observed in the high-temperature region. The increase in φ_0 below 30 K can be reasonably explained by the increase in the work function in the MnSi layer after its transition to the ferromagnetic state at ~ 30 K.

3.2 Magnetic-field-driven switching of current channels; magnetoresistive effect

What are the possibilities for controlling the transport properties of a structure provided by a magnetic field? The study of CVCs in a magnetic field H showed that for $T > 30$ K, the effect of the field is observed only for currents $I < I_{th}$. The action of H in this current region is completely determined by magnetoresistive properties of a manganite film. The magnetoresistance is negative, and its value is independent of the current being measured, which is typical for manganites. For $I > I_{th}$, the switching effect is observed, and the current begins to flow predominantly over the lower layer of the structure. Because MnSi does not have a noticeable magnetoresistance and the current through tunnel junctions for $T > 30$ K is independent of H, the magnetoresistive effect is not observed for $I > I_{th}$. For $T < 30$ K, a ferromagnetic order appears in the MnSi layer, and the structure already becomes a magnetic tunnel junction. The current through such a junction depends on the mutual orientation of respective magnetizations $\mathbf{M}_M$ and $\mathbf{M}_S$ in the LSMO and MnSi layers. Figure 12a demonstrates that the negative magnetoresistance for $I < I_{th}$ is preserved below 30 K, but a strong effect of H is also observed in the CVC part corresponding to $I > I_{th}$. At $T = 10$ K, the CVC becomes virtually linear already in the field ~ 1 kOe (Figs 12b, c). This can be interpreted as reverse switching of the current channel from the lower to the upper structure layer due to a decrease in the tunnel current in the magnetic field.

It follows that a few options exist for controlling the switching of current channels in a magnetic tunnel structure in the CIP geometry. The bias current causes the switching of the current channel from the upper to the lower layer of the structure, while the external magnetic field produces the reverse switching. The latter leads to the positive magnetoresistance effect in the magnetic tunnel structure with an absolutely new mechanism, which has not been considered previously. This mechanism determines the main features of the effect: the positive magnetoresistance is induced by the bias current, whose value increases upon increasing the bias current (it is known that the TMR effect is usually rapidly suppressed with increasing bias). The magnetoresistance can

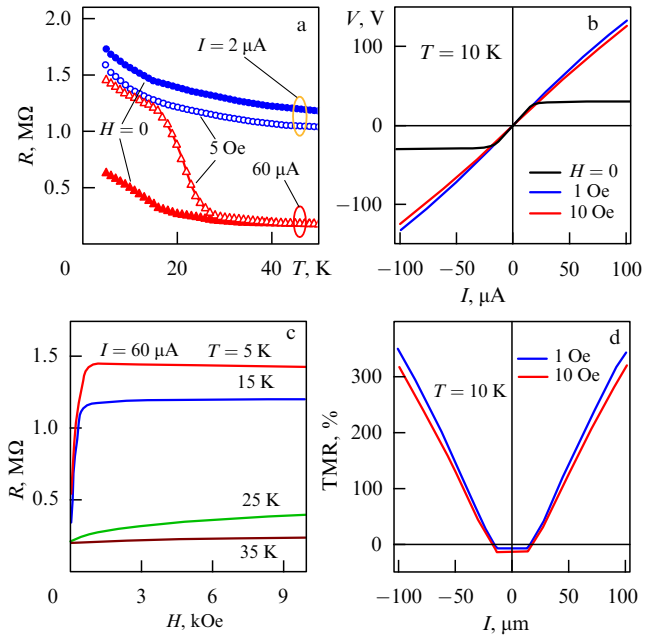

Figure 12. The $LSMO/LSM_{1-\delta}O/MnSi/SiO_2$ structure in the CIP geometry: (a) temperature dependences of the resistance for two bias currents, above and below the threshold current I_{th}; (b) CVC without a magnetic field and in fields 1 and 10 kOe; (c) dependence of the resistance on the magnetic field for the current $I = 60$ μA at different temperatures; (d) dependence of the magnetoresistance on the bias current through the structure.

reach 350% and no saturation of the effect was observed in the described experiments (Fig. 12d).

In considering the dependence of the tunnel current on the mutual orientation of magnetizations of ferromagnetic electrodes, we should probably assume that there are various types of ferromagnets in this case: the LSMO is a MASC ferromagnet, while MnSi should be assigned to MISC ferromagnets (which is confirmed in principle by electron state density calculations [55]). Only in this case is the tunnel junction resistance for the parallel orientation of magnetizations of electrodes greater than that for the antiparallel orientation [56]. In the absence of a magnetic field, due to the magnetostatic interaction, $\mathbf{M}_M$ and $\mathbf{M}_S$ are aligned antiparallel, the tunnel junction resistance is minimal, and, for $I > I_{th}$, the current flows over the lower layer in the structure. The magnetic field tends to align $\mathbf{M}_M$ and $\mathbf{M}_S$ parallel, the junction resistance increases, exceeding R_M, and even for $I > I_{th}$ the current begins to flow mainly over the upper layer of the structure with a linear CVC.

We have thus demonstrated that under certain conditions, the magnetic tunnel structure in the CIP geometry reveals absolutely new manifestations of spin-dependent electron transport. It becomes possible to perform the switching of current channels between conducting layers of a structure separated by a potential barrier. This switching can be controlled with the help of the bias current and magnetic field. The switching gives rise to a magnetic-field-driven nonlinear CVC and the magnetoresistance controlled by both the bias current and the magnetic field. An important factor was the choice of the manganite material for the tunnel structure, which provided the original technological method for fabricating a structure with the specified properties of the required quality and also the high spin polarization of at least one of the electrodes.

We also note that the new magnetoresistance mechanism found in the magnetic tunnel structure in the CIP geometry allowed us to propose a new magnetoresistive element for practical applications [57].

4. Cooperative systems of manganite-based magnetic tunnel junctions

4.1 Ferromagnetic granular materials as cooperative systems of magnetic tunnel junctions

Another attractive aspect of recent investigations is the manifestation of spin-dependent tunneling effects in a cooperative system, i.e., a system consisting of many identical magnetic tunnel junctions. One of the obvious advantages of such systems is the possibility of a simple amplification of spin-dependent electronic effects. On the other hand, we can expect the appearance of new effects characteristic only of cooperative systems. For example, it is well known that an ordered collective dynamic state can appear under certain conditions in complex systems, a classic example being the self-synchronization of oscillations in a large system of interacting Josephson junctions [58].

Promising materials for studying phenomena caused by the spin-dependent electron transport in cooperative tunnel systems are granular magnetic materials in which ferromagnetic granules with metallic conductivity are separated by thin insulating boundaries. These boundaries play the role of tunnel barriers, thereby forming a branched network of magnetic tunnel junctions. The resistance of such a system depends on the magnetization direction in granules near the junctions.

The authors of [59] were the first to propose the mechanism of intergranular spin-dependent tunneling for explaining the transport properties of ferromagnetic granular systems. The most complete theoretical explanation of the magnetoresistive effect related to intergranular tunneling was presented later in [60]. The authors applied their theory to explain the features of the magnetotransport properties of a granular ferromagnetic Ni film. The model takes an additional exchange energy into account, the one appearing when the magnetic moments of neighboring granules are nonparallel, and also uses the fact that the electron spin is preserved during tunneling between granules. If only linear terms are kept in the expansion of the magnetic energy, the magnetoresistance is given by

$$\frac{\Delta\rho}{\rho_0} = -\frac{PJ}{4k_B T}\left[M^2(H,T) - M^2(0,T)\right], \qquad (9)$$

where J is the exchange constant, P is the electronic polarization of a metal, and M is the magnetization. This model can therefore predict both the temperature and field dependences of magnetoresistance in granular magnetic films, actually representing a cooperative system of magnetic tunnel junctions.

4.2 Manganite-based granular materials: microstructure

The magnetoresistive effects observed in granular nickel samples considered above are weak, no more than a few percent. This is explained by the fact that the polarization degree P for conduction electrons in Ni does not exceed 11%. Therefore, it is not by accident that the renewed interest in spin-dependent transport effects in ferromagnetic granular media is associated with manganites.

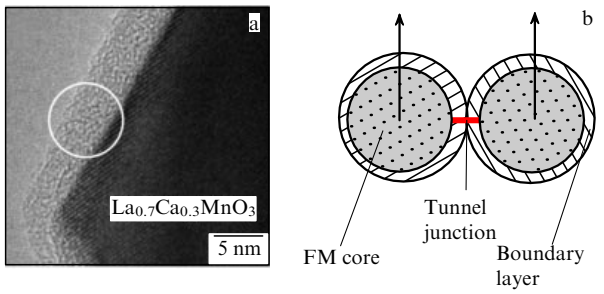

Figure 13. (a) Transmission electron microscope image of an $La_{0.7}Ca_{0.3}MnO_3$ granule; a thin disordered boundary layer always forming on the surface is clearly seen. (b) Explanation of the formation of magnetic tunnel junctions in a polycrystalline manganite sample.

Indeed, as we know already, the spin polarization P in ferromagnetic manganites can reach almost 100%, which can considerably enhance spin-dependent effects compared to granular materials based on 3d metals. In addition, it was found that intergranular tunnel junctions are naturally produced in manganites. Indeed, our electron microscopy studies [61] and investigations by other authors show that both bulk and film polycrystalline manganite samples have the required granular microstructure [62–64]. Each conducting ferromagnetic granule has a pronounced surface layer (Fig. 13a) whose structure and properties differ from those in the bulk of the granule. It is assumed that the surface layer is not ferromagnetic and has insulating properties. The thickness of the boundary layer ranges from 1 to 5 nm, depending on the manganite composition and synthesis conditions; therefore, if granules in a sample touch one another, the boundary layers play the role of a tunnel barrier between conducting granules, and a magnetic tunnel junction is formed in the contact region (Fig. 13b). The resistance of such a junction depends on the mutual orientation of magnetizations $\hat{\mathbf{m}}_i$ and $\hat{\mathbf{m}}_j$ of granules in the contact region:

$$R_T = R_{\uparrow\uparrow} + \frac{1}{2}\,(R_{\uparrow\downarrow} - R_{\uparrow\uparrow})(1 - \hat{\mathbf{m}}_i \times \hat{\mathbf{m}}_j)\,. \qquad (10)$$

Here, $R_{\uparrow\uparrow}$ and $R_{\uparrow\downarrow}$ are the junction resistances for the parallel and antiparallel orientations of magnetizations; R_T is maximal for the antiparallel orientation and minimal for the parallel orientation of magnetizations of granules in the contact region. The total magnetoresistance of a granular sample is determined by the total contribution from the network of magnetic tunnel junctions, taking into account that the granule magnetization directions are randomly distributed in the absence of a magnetic field.

4.3 Manganite-based granular materials: tunnel magnetoresistance

The mechanism of spin-polarized intergranular tunneling in manganites was first used to explain the magnetoresistive properties of a polycrystalline $La_{2/3}Sr_{1/3}MnO_3$ sample in [65]. Experimental studies have shown that along with the colossal magnetoresistance effect, which is observed near the magnetic phase transition, polycrystalline samples also reveal an additional contribution to the magnetoresistance at low temperatures. This contribution is negative, is saturated in low magnetic fields, and rapidly decreases with increasing the temperature. As a rule, it is not observed above 200 K and is absent in single crystals. The low-field magnetoresistance is

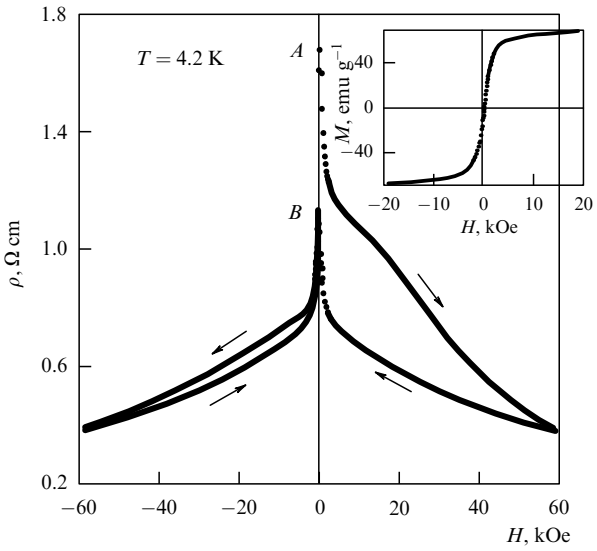

Figure 14. Dependence of the resistance of a polycrystalline $La_{0.7}Ca_{0.3}MnO_3$ sample on the magnetic field at 4.2 K; the inset shows the magnetization curve of the sample obtained at the same temperature.

explained in principle by the spin-dependent tunneling between ferromagnetic granules. When a magnetic field is applied, magnetic domains in the region of granule contacts (tunnel magnetic junction) rotate, which affects the tunnel probability of charge carriers and hence the resistance of the tunnel junction. It may seem that the resistance should change until the magnetization reaches saturation, i.e., when the sample is completely magnetized. However, it was found that the resistance changes slowly in large magnetic fields as well when the sample can be considered magnetized to saturation; the typical behavior is shown in Fig. 14 [66]. This change is probably related to the magnetic nature of surface layers of granules playing the role of potential barriers. We return to this question in what follows.

We briefly consider the reasons behind the formation of surface layers on manganite granules and their properties. The appearance of surface layers with properties drastically different from those of the bulk material has a few explanations.

(i) The manganite composition on the surface can differ from the rated composition, for example, due to oxygen nonstoichiometry; it is well known that the electric and magnetic properties of manganites very strongly depend on the composition [13].

(ii) The crystalline structure on the surface experiences additional stresses, and dislocations can appear.

(iii) The Mn–O–Mn bonds on the surface are distorted and broken, resulting in a suppression of the ferromagnetic exchange interaction on the surface (double exchange) and the appearance of an insulating state.

All these reasons affect the properties of the surface layer, producing defects in them and making them disordered. The electronic and magnetic properties of surface layers strongly depend on many factors such as the material composition, fabrication technology, and processing conditions. We note that a surface layer not only forms the potential barrier but also determines the character and strength of intergranular interactions and therefore the dependences of the magnetization of granules and the resistance of samples on the magnetic field.

The tunneling mechanism of the resistance and magnetoresistance in polycrystalline manganites has been studied by different research groups. The dependences on the nature of the surface layer, the granule size and porosity, and the relation between magnetic and transport properties were investigated in [62–70]. The aim of these studies was to develop controllable cooperative systems of magnetic tunnel junctions with prescribed magnetoresistive properties in weak magnetic fields, which could open up prospects for practical applications of such systems.

Technology developed in recent years allows controlling granule sizes in manufactured samples, synthesizing samples with an ordered microstructure, and changing the properties of potential barriers in a controllable way. The dependences of tunnel conduction and tunnel magnetoresistance in granular manganite samples on the height and thickness of the potential barrier can be analyzed using a simple phenomenological model. We consider this model. The conduction G_s of a single tunnel junction is usually described by the Simmons model [7]. In the low-voltage approximation with a rectangular potential barrier, this model gives the dependence

$$G_s(V) = \cos^2\left(\frac{\theta}{2}\right)\left[G_0 + G_1 V^2\right], \tag{11}$$

where the term $\cos^2(\theta/2)$ takes the spin-dependent tunneling into account, assuming a 100% polarization of charge carriers in the granules, and θ is the angle between magnetizations of ferromagnetic granules forming a tunnel transition. Constants G_0 and G_1 are related to the height φ and thickness s of the barrier as

$$\begin{aligned} G_0(\beta, s) &= \frac{3.1\times 10^{10}}{s^2}\,\beta e^{-\beta}, \\ G_1(\beta, s) &= \left(\frac{1}{192\beta} - \frac{1}{64\beta^2} - \frac{1}{64\beta^3}\right) 6.84\times 10^{10} s^2 e^{-\beta}, \end{aligned} \tag{12}$$

where $\beta = 1.025 s\sqrt{\varphi}$, G_0 is expressed in Sm cm^{-2}, G_1 in Sm cm^{-2} B^{-2}, s in Å, and φ in eV; and β is a parameter determining the probability of tunneling through the potential barrier.

In the case of polycrystalline materials, it is necessary to introduce an additional parameter — the number of barriers making an efficient contribution to the resistance. This corresponds to the conduction distribution in a sample. If λ is the fraction of tunnel contacts between granules (separated by a distance l) contributing to the voltage drop across the sample, expression (11) for the conduction of a single tunnel junction is modified to

$$G(V) = \left\langle \cos^2\left(\frac{\theta}{2}\right)\right\rangle \left[\frac{G_0}{\lambda l/D} + \frac{G_1}{(\lambda l/D)^3}\, V^2\right]. \tag{13}$$

This equation relates the conduction G to the voltage drop V for the whole granular sample. For the whole sample, the factor responsible for spin-dependent tunneling in (11) should be replaced, of course, with its value averaged over all tunnel junctions. In reality, this factor is responsible for the temperature and magnetic-field dependences of the magnetoresistance. Assuming that anisotropy axes in a granular sample are oriented randomly, we can use the relation $\langle\cos^2(\theta/2)\rangle = 0.5$ in the absence of a magnetic field. The barrier thickness s is twice the thickness t of the surface layer of granules ($s = 2t$).

Using this rather simple model, it is possible to estimate the basic parameters of a cooperative system — the mean height φ and mean thickness s of tunnel barriers in a sample — quite accurately. On the other hand, by specifying the basic parameters of tunnel barriers (granule interfaces) at the technological stage, we can obtain the required behavior of tunnel magnetoresistance in a cooperative system of magnetic tunnel junctions. For example, the authors of [67] have managed to change the properties of granule boundaries by using different technological approaches without changing the mean diameter (~ 30 nm) of the granules. The study of a series of samples with different φ showed that the low-field magnetoresistance is similar for all samples in the series. This result suggests that φ is not the main parameter determining the behavior of the low-field magnetoresistance.

Other technological approaches can be used to control the size of granules. For example, the sol–gel method was used to produce polycrystalline manganite samples with varying granule sizes above 14 nm [62]. Comparative studies of samples with different granule sizes revealed some typical characteristics. As the granule size decreases, the thickness of the surface layer of the granules increases, and the polydomain granule magnetization mode becomes single-domain. This drastically changes the response of the magnetization and magnetoresistance to the magnetic field.

In addition, these studies have shown that the magnetic state of the surface layer of granules, i.e., the magnetic properties of the potential barrier, play a considerable role in the mechanism of tunnel magnetoresistance. It is assumed that the spin moments of Mn ions in a disordered surface layer are frozen in random directions (as in spin glass) due to the random distribution of exchange interactions and anisotropy, which increases the probability of magnetic scattering of tunneling charge carriers with the specified spin polarization even if the magnetizations of granules are already parallel. The external magnetic field tends to align the frozen moments of ions parallel to each other, resulting in an increase in the electron tunneling probability without the loss of the spin state. It is obvious that to magnetize such a spin-glass state in the surface layer, high magnetic fields are needed, greatly exceeding ferromagnetic saturation fields determined by the magnetization of granule volumes. That is why, along with the low-field magnetoresistive effect caused by magnetization of granules forming a tunnel junction, high-field magnetoresistance is observed (Fig. 14), related to the magnetization of granule boundaries.

The relation between magnetization processes and the magnetoresistance can be described in the general form by expression for the conduction σ of polycrystalline manganites in a magnetic field H [68]:

$$\frac{\sigma}{\sigma_0} \sim 1 + 2\mathbf{M}\langle\hat{\mathbf{s}}_b\rangle + \left\langle(\mathbf{M}\,\hat{\mathbf{s}}_b)^2\right\rangle, \tag{14}$$

where σ_0 is the conduction in zero magnetic field, $\hat{\mathbf{s}}_b$ is the spin orientation of a magnetic center in the surface layer of a granule, and $\mathbf{M}$ is the normalized bulk magnetization of granules. In strong fields, Eqn (14) becomes

$$\frac{\sigma}{\sigma_0} \sim 1 + \frac{1}{3}\,M^2 + 2\chi_b HM, \tag{15}$$

where χ_b is the magnetic susceptibility of the granule surface layer. Knowing its behavior, we can predict the temperature and field dependences of the tunnel magnetoresistance in strong magnetic fields.

It seems that the surface layer of granules cannot always be assumed to be ordered. By studying magnetic and magnetotransport properties of $(La_{0.5}Eu_{0.5})_{0.7}Pb_{0.3}MnO_3$ manganites in single-crystal and polycrystal states, we observed the formation of an ordered phase on the surface of granules in polycrystals at the technological stage [69]. Magnetic and heat capacity measurements show that this phase has the temperature of transition to the antiferromagnetic state near 40 K. The behavior of the magnetoresistance changes at the same temperature. In particular, the field dependences of the resistance below 40 K exhibit a pronounced hysteresis. All this can be explained assuming that the transport properties of a polycrystal at low temperatures are determined by spin-dependent tunneling between granules, while the potential barrier formed by surface granular layers is in the paramagnetic state above 40 K and in the antiferromagnetic state below 40 K. Thus, a network of magnetic tunnel ferromagnetic metal–antiferromagnetic dielectric–ferromagnetic metal junctions is formed in the sample.

The possibility of the formation of a boundary layer of granules with antiferromagnetic ordering of the moments of Mn ions due to oxygen nonstoichiometry was discussed in [70]. As regards the conduction of magnetic tunnel junctions with an antiferromagnetic potential barrier, this nontrivial problem is generally complicated by many details. One of the options for solving this problem for a single junction can be found in [71].

The idea of controlling the properties of potential barriers in a cooperative system of magnetic tunnel junctions was implemented in the study of manganite-based composite materials. Indeed, if the main phase of the composite, manganite, is a system of granules, while the second, minor phase fills the intergranular space, thereby forming potential barriers between granules, then, by selecting the composition of the second phase, we can produce materials with specified magnetoresistive properties. In addition, the choice of the second phase affects the character of magnetic intergranular interactions, i.e. the magnetic properties of the composite and the field dependence of magnetoresistance.

The study of composites consisting of $La_{0.7}Sr_{0.3}MnO_3$ and borosilicate glass with different weight contents showed an improvement in magnetoresistive properties in weak magnetic fields compared to single-phase $La_{0.7}Sr_{0.3}MnO_3$ [72]. The scanning electron microscopy and X-ray diffraction studies of the microstructure of composites showed that glass forms sharp boundaries between LSMO granules, without any mixing. The authors observed a considerable increase in the low-field magnetoresistance (at 200 Oe) for the optimal composition containing 25 wt.% borosilicate glass. The results were interpreted using a model in which glass layers separating manganite granules act as potential barriers for the spin-polarized tunneling of charges between granules.

Some other attempts were also made to create artificial barriers between granules by introducing dielectric phases in polycrystalline manganite. The study of $La_{0.7}Sr_{0.3}MnO_3 - CeO_2$ [73] and $La_{0.7}Ca_{0.3}MnO_3 - SrTiO_3$ [74] composites has also demonstrated an increase in the low-field tunnel magnetoresistance with increasing the concentration of the dielectric phase. It is interesting that the maximum of this effect is observed at concentrations close to the percolation threshold for the conducting phase of manganite. Composites with magnetically ordered dielectric phases were also studied: $(1 - x)La_{0.7}Pb_{0.3}MnO_3 - xPr_{0.63}Ca_{0.37}MnO_3$, in which praseodymium manganite is a dielectric with the antiferromagnetic ordering below $T_N = 175$ K [75], and $La_{1-x}Sr_xMnO_3 - Fe_3O_4$ [76]. In the latter case, it is interesting that Fe_3O_4 is a ferromagnetic oxide that has a rather large conduction at high temperatures due to the hopping mechanism (hops between Fe^{2+} and Fe^{3+} ions) and which becomes a dielectric below the Verway temperature $T_V = 120$ K due to transition to the charge-ordered state. In both cases, an increase in the low-field magnetoresistance was observed in the region of low concentrations of the added phases, but no specific features related to the phase transition temperatures for these phases were found. The authors assumed that the change in the magnetoresistance was mainly caused by the formation of defects on the boundaries of granules in the main phase during the addition of the minor phase.

To summarize the discussion of spin-polarized tunneling in granular manganite materials, we conclude that interest is attracted to fundamental features of the observed phenomena and technological aspects of fabricating systems containing many magnetic tunnel contacts. Although appreciable effects are currently observed only at low temperatures, materials representing large ensembles of magnetic tunnel junctions have a great potential for applications. In addition, the magnetoresistive effect does not exhaust all the phenomena of spin-polarized electron transport in cooperative systems of magnetic tunnel junctions.

It is quite probable that phenomena related to the spin transfer effect can be discovered; for example, a polarized current can cause a reorientation of the magnetization of granules [77] or even their precession. Of course, certain conditions should be fulfilled; granules can be assumed to have a nanosize and the magnetic interaction among them should be very weak. Other manifestations of spin-polarized transport in a cooperative system of magnetic tunnel junctions are also possible. For example, such a system can detect microwave radiation due to the relation between the polarized current through tunnel junctions and the spin dynamics of granules induced by microwave radiation. We discuss this question in detail in the next section.

5. Response of a magnetic tunnel junction to microwave radiation; detecting properties of manganite-based tunnel junctions

5.1 Detecting properties of a classic (nonmagnetic) tunnel junction

We consider the response of tunnel junctions to the action of an electromagnetic field. We recall that a classical (nonmagnetic) tunnel junction gives a nonlinear response to the action of external fields up to frequencies in the visible range [78–81]. Investigations of detecting tunnel junctions in different frequency ranges have shown that the observed nonlinearity is exclusively related to the mechanism of electron tunneling through a potential barrier between two metals. This also concerns the operation of tunnel junctions as mixers of electromagnetic signals. Except for the sensitivity to electromagnetic radiation in a broad frequency range, a point contact demonstrates a high response speed, which is very important for practical purposes. This occurs due to the high velocity of electron tunneling through the potential barrier (estimates made for thin barriers [82] give 10^{-16} s) and an extremely small time constant (RC) due to the small size of the junction region for a point contact.

Results obtained in different experiments completely agree with the quasistatic theory of electron tunneling based on the classical Simmons model considered above. Expressions for the tunnel current obtained by Simmons in the free-electron approximation can be used even at high frequencies.

If the photon energy is smaller than the potential barrier height, then the interaction of a tunnel junction with radiation is mainly determined by the adiabatic modulation of the Fermi level in one metal electrode with respect to another. This modulation produced by fields inside the potential barrier causes the modulation of the effective voltage across the junction. The total voltage across the junction can be written in the form

$$V(t) = V_b + v(t)\cos(\omega t)\,, \tag{16}$$

where V_b is the bias voltage across the tunnel structure and $v(t)$ is the voltage across the structure induced by the electromagnetic field at the frequency ω. A constant component or the current rectified in the tunnel structure is determined, as usual, by averaging the current $J(t)$ over the period:

$$J_{rec} = (2\pi)^{-1}\int_{-\pi}^{\pi} J(t)\,\mathrm{d}(\omega t)\,. \tag{17}$$

It is obvious that a nonzero detecting voltage can be expected only in the presence of a bias voltage V_b or for an asymmetric CVC.

We note that the CVC nonlinearity should also determine the ability of a tunnel structure to convert radiation frequency — to mix signals with frequencies ω_1 and ω_2.

5.2 Detecting properties of a magnetic tunnel junction

There is good reason to believe that magnetic tunnel structures will exhibit principally new manifestations of the response to the action of a microwave field. Indeed, the detection of the microwave current in magnetic structures can be described by an absolutely new mechanism based on the relation between spin-dependent electron transport and spin dynamics. This was first demonstrated in [83]. Experiments were performed with a magnetic tunnel nanocontact fabricated such that one of the ferromagnetic layers played the role of an electrode with a fixed magnetization direction, while another layer played the role of an electrode with a free (unfixed) magnetization direction, which could be easily changed. The resistance of a magnetic tunnel junction depends on the relative orientation of the magnetization of the fixed and free layers. The authors showed that a weak microwave current passed through a magnetic tunnel nanocontact in a constant magnetic field can generate a constant voltage across the contact if the current frequency coincides with the spin oscillation frequency of the free electrode of the structure. This can be understood based on the following considerations: the current passing through a layer with a fixed magnetization becomes spin-polarized and, due to the spin-transfer torque effect, transfers the torque to the magnetic moment of the free ferromagnetic layer. When the frequency of an alternating current coincides with the magnetic resonance frequency for the free layer, its magnetization begins to precess. This leads to the appearance of a time dependence of the resistance [see expression (10)]: the structure resistance is different for the positive and negative polarities of the current, which leads to the diode effect, resulting in the rectification of the alternating current in the tunnel structure (Fig. 15).

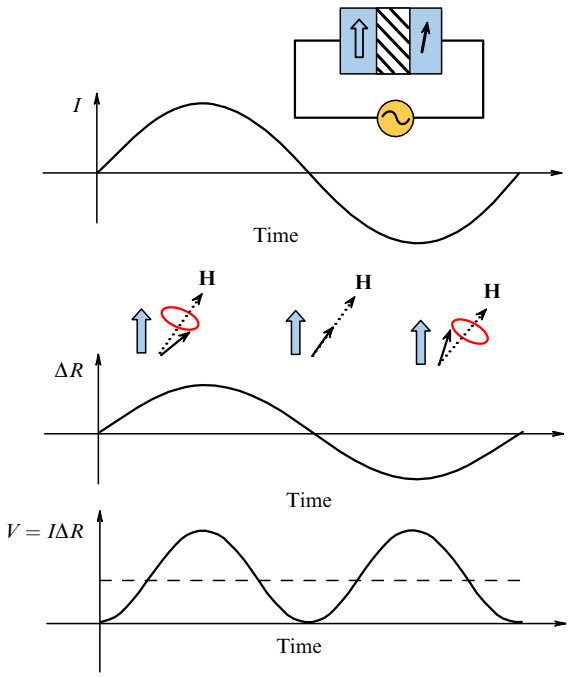

Figure 15. Explanation of the diode effect in a magnetic tunnel junction. When the frequency of an alternating current coincides with the eigenfrequency of a free FM layer, the layer magnetization begins to oscillate due to the spin transfer effect; the resistance of the structure is smaller for the negative alternating current than for the positive current because the angle between magnetizations of the free and fixed ferromagnetic layers in smaller is the first case than in the second one.

The difference in the resistance for the positive and negative current also determines the detection effect in a conventional semiconductor diode, but the mechanism is substantially different. In addition, unlike in a semiconductor diode, the noise of a new magnetic tunnel diode is weaker because a constant voltage is induced only in a narrow frequency range near the resonance frequency, which can be tuned by a magnetic field. In fact, we have a selective, magnetic-field-controlled microwave detector. We note that under certain conditions, the relation between the giant tunnel resistance and the spin-transfer torque effect in a ferromagnetic nanolayer leads to a negative differential resistance, resulting in amplification [5].

The resonance precession in the example considered above is induced by the microwave current, which is then detected. This mechanism imposes certain restrictions; in particular, the structure size should be a few nanometers. At the same time, a different situation is possible when the magnetization precession in the free layer is induced by a microwave field, as in the usual ferromagnetic resonance, and the same microwave field induces the microwave current through the structure [84]. In this case, for example, the restriction on the size of the tunnel junctions is removed. However, the mechanism is still based on the relation between the spin-polarized current and spin dynamics in a magnetic tunnel junction.

5.3 Detecting properties of a manganite-based magnetic tunnel junction in the 'current-in-pane' geometry

Studies of the response of manganite-based tunnel structures to microwave radiation have not been reported in the literature so far. Here, we briefly present the results of our

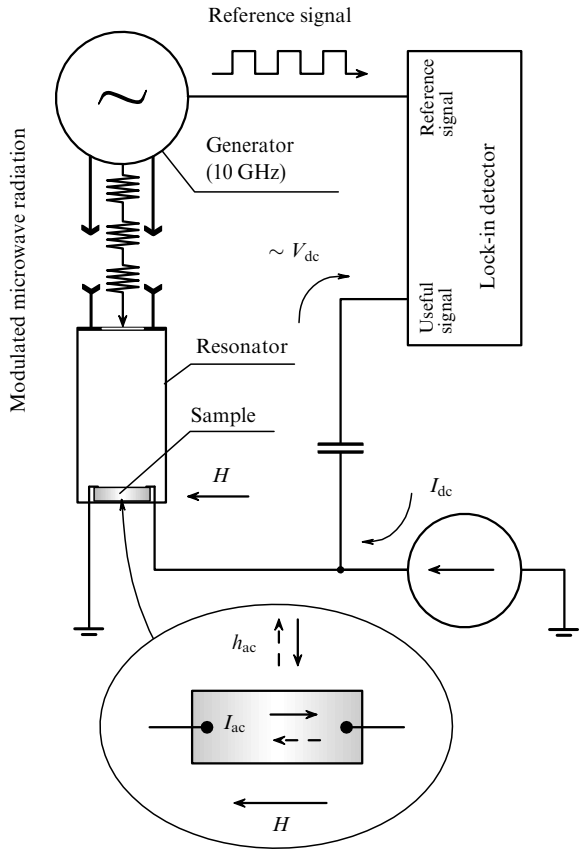

Figure 16. Schematic of the experimental setup for studying the magnetically controlled detection effect. The lower part of the figure shows the top view of the sample; H is the constant magnetic field, h_{ac} and I_{ac} are the high-frequency magnetic field and high-frequency surface current, respectively.

investigations of detecting the properties of the $LSMO/LSM_{1-\delta}O/MnSi$ structure in the microwave range; the transport properties of this structure in the CIP geometry were discussed in Section 2.2. We also used planar geometry in our experiments, measuring the rectified voltage at contacts formed on the upper layer of the structure.

The schematic of the experimental setup is shown in Fig. 16. The structure was placed inside a rectangular 10 GHz microwave resonator (the TE_{102} mode) into the antinode of a magnetic microwave field. The microwave field h_{ac} excited a magnetic resonance in the structure layers and induced a microwave current I_{ac} in the structure plane. We used modulated microwave radiation and synchronous detection. The electric circuit also provided a constant bias current I_{dc} applied to the structure.

Of course, we were primarily interested in the magnetically dependent microwave detection effect, which could be based on the relation between the spin-polarized electron transport and spin dynamics in the tunnel structure. Indeed, the structure reveals the detection effect, and the rectified voltage V_{dc} at temperatures below 30 K depends on the strength of the external magnetic field (Fig. 17a). The voltage value and the dependence of the effect on the magnetic field are essentially determined by the bias current in the structure. We note that the maximal effect and strongest changes in the magnetic field occur for a certain bias current I_{dc} when the maximal CVC nonlinearity is observed (Fig. 17b). Upon detuning from I_{dc}, the detection effect decreases in the smoother parts of the CVC, and the detection effect vanishes for the zero bias. It seems that the nonlinearity of the CVC determines the detecting properties of the structure. The dependence on the magnetic field appears due to a change in the CVC in the magnetic field; as the magnetic field increases, this dependence becomes smoother, tending to a linear dependence in the limit. As a result, the detection effect decreases with increasing the magnetic field. Hence, in this case, the detection mechanism is the same as in 'classical' tunnel junctions, although it is the dependence of the resistance of the magnetic tunnel junction on the magnetic field that determines the change in the CVC, as mentioned in Section 2.2.

The results presented above were obtained at temperatures near 30 K corresponding to the transition temperature of the lower conducting layer of the structure to the ferromagnetic state. This determines the comparatively weak dependence of the CVC of the structure on the magnetic field. It would seem that at low temperatures, the dependence of the effect on the field in weaker magnetic fields should be stronger. We see (Fig. 12b) that at $T = 10$ K, the CVC becomes almost linear already in magnetic fields about $H = 1$ kOe. Indeed, this is reflected in the behavior of the detection effect, which is not observed, in fact, above 1 kOe (Fig. 17b). We note that the noise level during the recording of the detected signal as a function of the magnetic field is rather high. This is probably related to the mechanism of changing the CVC of a tunnel structure in the CIP geometry in the magnetic field.

The change in the CVC is determined by a redistribution of current channels between the upper and lower layers of the structure controlled by magnetic tunnel junctions between current contacts. And while the area of single magnetic tunnel junctions in the CPP geometry is specified by the physical size, the junction area is not strictly bounded in our case and can be varied, in fact, arbitrarily. The junction area can be effectively changed by varying the bias current and the magnetic field. This is determined by the homogeneity of layers, the quality of interfaces, the domain structure of ferromagnetic layers, their magnetization processes, and other factors. In this case, the junction itself would have inhomogeneous properties, and each part of the junction would engage at different instants to the detection process to form a response to microwave radiation.

Under certain conditions satisfied by the structure in the CIP geometry, a mechanism based on the relation between the spin-polarized current and spin dynamics can be realized. This is confirmed, for example, by the magnetically dependent detection effect observed for the bias current $I_{dc} = 60$ μA (Fig. 17d). The CVC becomes smooth (nearly linear) in the field $H = 1$ kOe and ceases to change upon further increasing the field; based on the mechanism proposed above, the microwave response should not be observed. Nevertheless, the signal is observed in fields much higher than 1 kOe; the high noise level can again be explained by the specific features of the 'operation' of magnetic tunnel junctions in the CIP geometry. The irregular dependence of V_{dc} on the magnetic field in the mechanism related to the magnetic dynamics can be explained by the fact that at low temperatures, manganites have very broad magnetic resonance lines, typically representing a superposition of several absorption lines. However, it is currently difficult to make more certain conclusions about detection mechanisms rea-

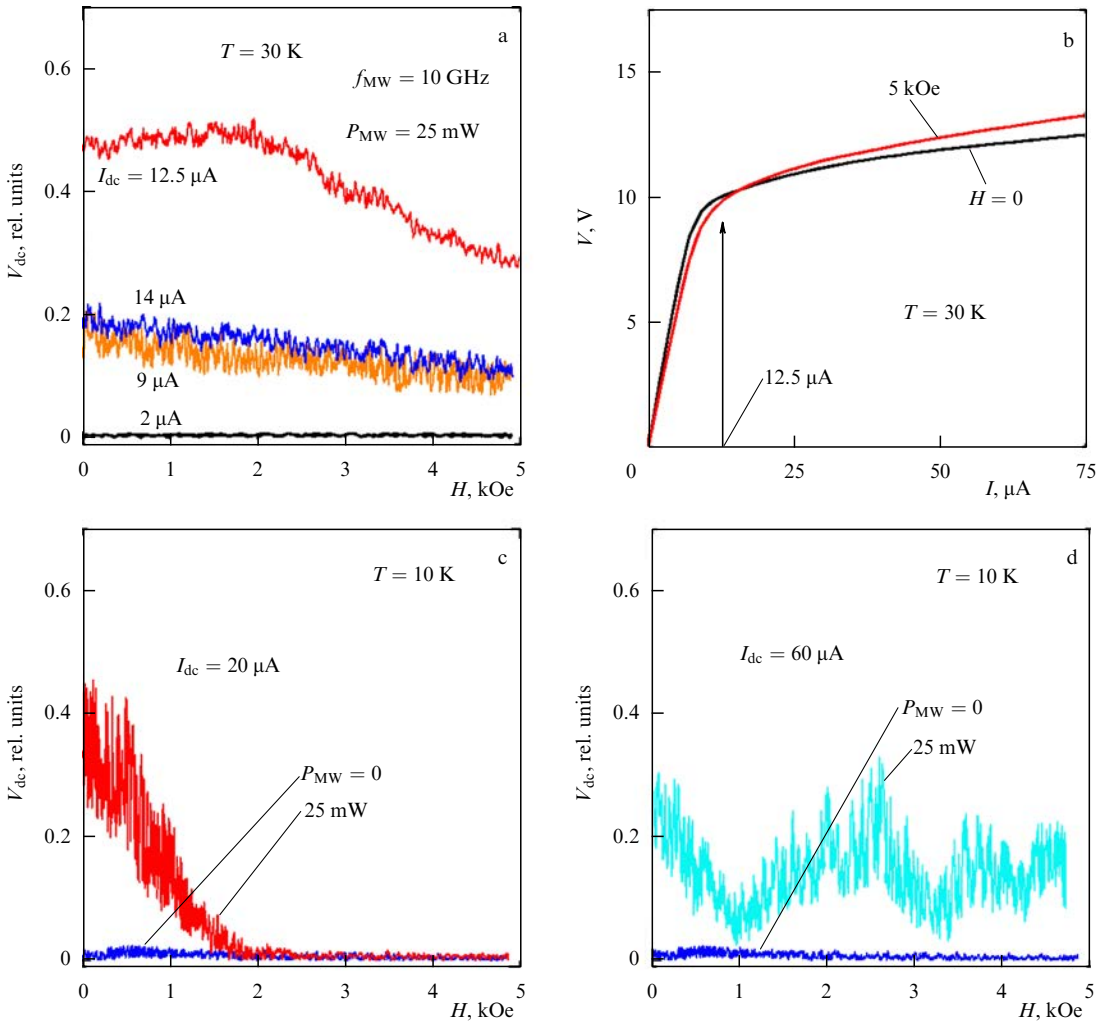

Figure 17. The LSMO/$LSM_{1-\delta}O$/MnSi/SiO_2 structure in the CIP geometry: (a) dependences of the detected voltage V_{dc} on the magnetic field H for different bias currents I_{dc}, $T = 30$ K; (b) VAC of the structure without a magnetic field and in the field 5 kOe, $T = 30$ K; (c) V_{dc} as a function of H for $T = 10$ K and $I_{dc} = 20$ μA; (d) V_{dc} as a function of H for $T = 10$ K and $I_{dc} = 60$ μA. f_{MW} and P_{MW} are the frequency and power of microwave radiation.

lized at high bias currents, and additional investigations are required, in particular, of structures with other compositions.

5.4 Magnetically dependent detection of microwave radiation in a cooperative system of manganite-based magnetic tunnel junctions

The effects of the magnetically controlled detection of microwave radiation in single magnetic tunnel junctions give promise that similar effects controlled by the same mechanisms will also be observed in cooperative systems of magnetic tunnel junctions. We note that in this case, as mentioned above, not only the usual summation of effects from individual junctions but also the amplification of the effect, for example, due to synchronization, is possible.

For the reasons considered in Section 3.3, convenient objects for study are granular manganites, actually representing a branched network of magnetic tunnel junctions with a large tunnel magnetoresistance. Using the method described in the preceding section (see Fig. 16), we indeed discovered a magnetically dependent contribution to the constant voltage in a granular $La_{0.7}Ca_{0.3}MnO_3$ manganite sample induced by microwave radiation [85, 86]. Figure 18a shows the typical dependences of the detected voltage on the magnetic field obtained at different microwave frequencies (here, we used a short-circuited waveguide instead of a resonator to perform studies at different frequencies). The dependences have a form resembling a magnetic resonance absorption line. The maximum of the dependences shifts upon changing the radiation frequency, as can be expected for a ferromagnetic resonance line. This suggests that a mechanism related to the magnetic dynamics in magnetic tunnel junctions of the system is indeed involved in this case.

The principal details of the detection mechanism in a cooperative network of junctions can be conveniently considered by the example of a single tunnel contact formed by neighboring ferromagnetic granules separated by a thin insulating boundary (Fig. 18b). Each of the grains is characterized by its own coercive force and hence by different magnetic resonance conditions. We assume that for a certain magnetic field directed along the current trajectory, the magnetic moment of the ith granule is fixed at an angle α to the field direction, while the jth granule is in resonance conditions and its moment precesses at a frequency f. According to (10), this precession leads to a time dependence of the resistance $R_T = R(t)$. If the equilibrium direction is defined as $\hat{\mathbf{m}}_i = (\hat{\mathbf{e}}_x \cos\phi + \hat{\mathbf{e}}_y \sin\phi)\sin\alpha + \hat{\mathbf{e}}_z \cos\alpha$ (where ϕ is the angle between the projection of $\hat{\mathbf{m}}_i$ onto the xy plane an $\hat{\mathbf{e}}_x$), then $\hat{\mathbf{m}}_j$ oscillates as $\hat{\mathbf{m}}_j = (\hat{\mathbf{e}}_x \cos(2\pi ft) + \hat{\mathbf{e}}_y \sin(2\pi ft)) \times \sin\theta + \hat{\mathbf{e}}_z \cos\theta$

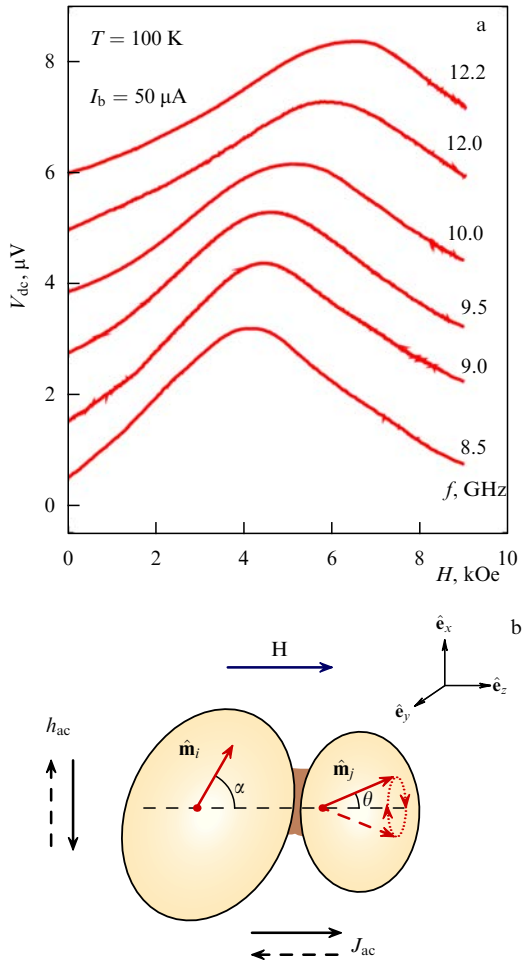

Figure 18. (a) Dependence of the direct-current voltage V_{dc} detected on a polycrystalline $La_{0.7}Ca_{0.3}MnO_3$ sample on the magnetic field; the dependences shown for different microwave frequencies f are displaced along the ordinate for clarity; the bias current through the sample is $I_b = 50$ μA and $T = 100$ K. (b) Schematic drawing of a contact of two ferromagnetic granules explaining the magnetically dependent mechanism of detection of microwave radiation.

(θ is the precession angle). Because the high-frequency magnetic field h_{ac} also induces the high-frequency current $I(t) = I_{ac}\sin(2\pi ft - \delta)$ (where δ is the possible phase shift between oscillations of $\hat{\mathbf{m}}_j$ and I), the rectified voltage

$$V_{dc} = \langle I(t)\, R(t)\rangle_T = \frac{I_{ac}(R_{\uparrow\downarrow} - R_{\uparrow\uparrow})}{4}\sin\theta\,\sin\alpha\,\cos(\phi - \delta) \quad (18)$$

appears across the sample.

The microwave detection mechanism described above is similar to that proposed in [83] to explain the diode effect in a single magnetic tunnel junction; in that case, however, the resonance oscillation of the magnetization of a free electron in a tunnel junction was excited not by a microwave field but by a high-frequency spin-polarized current flowing through the junction.

The proposed model is quite reasonable, but, no doubt, the physical picture of a random network of magnetic tunnel junctions realized in a granular material is more complicated. Magnetic tunnel junctions in this system are not identical and their characteristics are described by distribution functions. These functions determine the final dependence of the rectified voltage on the magnetic field. Nevertheless, expression (18) qualitatively explains the dependences of the detection effect on the temperature, the microwave frequency and power, and the bias current through a sample [85, 86].

We note in conclusion that a manganite-based granular material is a simple microwave detector with magnetic-field-controlled sensitivity [87].

6. Effect of electromagnetic radiation on the transport properties of magnetic tunnel structures; photoelectric phenomena

6.1 Photoelectric response of a classic (nonmagnetic) tunnel junction

Obviously, a quite different response of a tunnel structure to electromagnetic radiation should be expected if the photon energy $h\nu$ exceeds the height φ_0 of the potential barrier of the structure. Two basic processes can be distinguished here. The first is photoemission. The light absorbed by a metal (an electrode) excites electrons to energy levels that are high enough to overcome the potential barrier. If voltage is applied to the structure, then, along with the tunnel current, a photocurrent determined by photoexcited electrons appears. The threshold of this process is the barrier height φ_0, the difference between the Fermi levels of the metal and the edge of the conduction band of the dielectric. In the simplest case, with the scattering and relaxation processes neglected, the photoemission current (photocurrent) is described the Fowler relation [88]

$$J_{ph} = C(h\nu - \varphi_0)^2 \quad \text{for} \quad h\nu > \varphi_0\,. \quad (19)$$

Although this relation is very useful for the description of the main properties of the photocurrent in a tunnel structure, it neglects many features of the photoemission process [89]: (i) The electron distribution in the metal at a finite temperature is spread above the Fermi level; (ii) the electron scattering in the conduction band of the metal and the dielectric plays a certain role; (iii) the quantum mechanical transmission coefficient $T(\varepsilon)$ of the barrier in not unity for $\varepsilon > \varphi_0$, and therefore part of the electrons are reflected from the barrier; (iv) the barrier height can depend on the stress in the structure, which is determined by the influence of specular reflection forces, and even on the radiation intensity, for example, due to effects caused by a volume charge; (v) the absorption of light in the metal leads to the dependence of the photocurrent on the electrode thickness; in addition, if the thickness of the first electrode (from the irradiation side) is small, the light can reach the second electrode, exciting carriers in it and thereby producing its own contribution to the photoemission current though the structure; and (vi) the photocurrent considerably depends on electron–electron and electron–phonon interactions. Resolving the question of which of the above-mentioned factors plays a dominant role and which are of secondary importance requires detailed studies for each particular structure.

It is interesting that studies of photoemission effects in tunnel structures in the 1970s were extensively used for determining their electronic properties [90, 91]: the height and shape of the potential barrier, the charge distribution in a dielectric, the topographic distribution of the barrier height, the distribution of traps inside the barrier, the mean free path, and energy losses of carriers.

The photoelectric response of a tunnel structure can be caused, apart from photoemission, by another process. Light

with the photon energy hv exceeding the energy gap E_g of an insulator playing the role of the potential barrier of the structure can generate electron–hole pairs. If the recombination rate is not too high, the electrons and holes can make a considerable contribution to the photocurrent through the tunnel junction. Obviously, the generation of electron–hole pairs also has a threshold and can occur only for $hv \geqslant E_g$.

Thus, the spectral dependence of the photoresponse of a tunnel structure is determined by two contributions. The value of each of the contributions depends on the topology and energy structure of each of the layers of a particular tunnel junction. These factors also determine the kinetic behavior of the photocurrent.

6.2 Effect of optical irradiation on the transport properties of a manganite-based magnetic tunnel structure

The possibility of controlling the transport and magnetotransport properties of magnetic tunnel junctions by optical radiation is, of course, quite attractive. This concerns not only the manganite-based tunnel structures discussed in this review, but also magnetic tunnel structures as a whole. We consider the original study of the photoelectric response of the $LSMO/LSM_{1-\delta}O/MnSi$ manganite-based magnetic tunnel structure in the CIP geometry [92].

Photoinduced changes in the transport properties of the structure in the planar geometry are reversible and tend to saturate upon increasing the optical radiation power. Typical changes in the CVC caused by optical radiation are shown in Fig. 19a. Figure 19b demonstrates the photoinduced change in the voltage across the structure as a function of the optical radiation power. The dependence of the magnetoresistive effect of the structure on the optical radiation power is shown in Fig. 19c. We can see that photoinduced changes rapidly saturate at comparatively low optical powers and do not change with a further increase in power. This suggests that the observed changes are not caused by the trivial heating of the structure due to light absorption. This is also confirmed by the spectral dependence of the photoelectric effect shown in Fig. 20a. The dependence has a threshold, and changes in the transport properties are observed only for optical radiation with the photon energy exceeding $(hv)_{th} \approx 1.17$ eV.

Analysis of spectral dependences shows that the photoelectric effect is related to the interband absorption of light in an insulating layer of the structure, accompanied by the formation of an electron–hole pair (Fig. 20b), but not to the photoemission of electrons from metal electrodes. First, because the role of the insulating layer in the structure is played by a manganese-depleted nonmagnetic LSMO layer, its energy gap can be estimated from the data for $La_{0.7}Sr_{0.3}MnO_3$ in the paramagnetic state, according to which $E_g \approx 1$ eV [93], which approximately coincides with $(hv)_{th}$. Second, our estimates [49] show that the mean value of

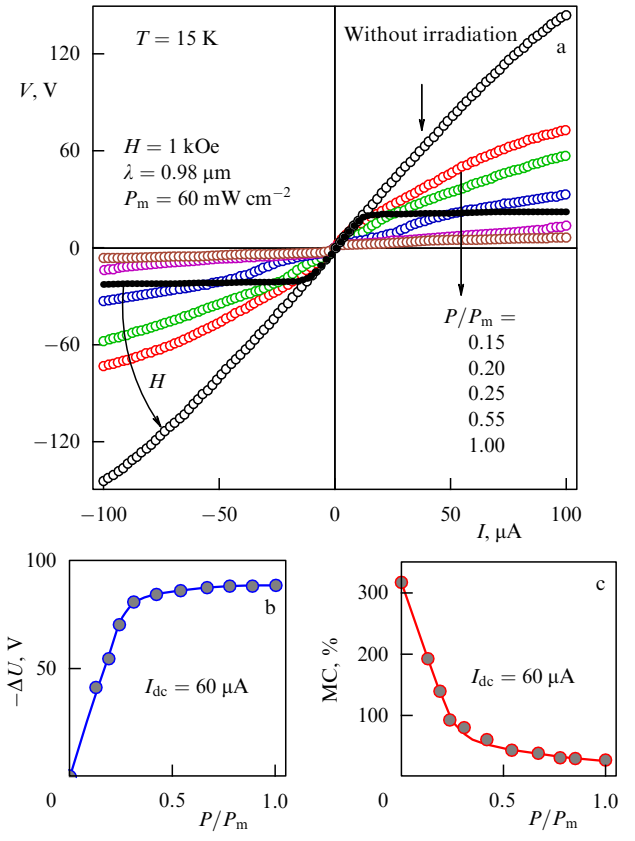

Figure 19. The $LSMO/LSM_{1-\delta}O/MnSi/SiO_2$ structure in the CIP geometry. (a) CVC of the structure; shown are the dependences without irradiation for $H = 0$ and 1 kOe and for different optical powers in a magnetic field. (b) Photoinduced change in the voltage across the structure as a function of the optical radiation power for $I_{dc} = 60$ μm. (c) Photoinduced change in the magnetoresistive effect in the structure as a function of the optical radiation power for $I_{dc} = 60$ μA.

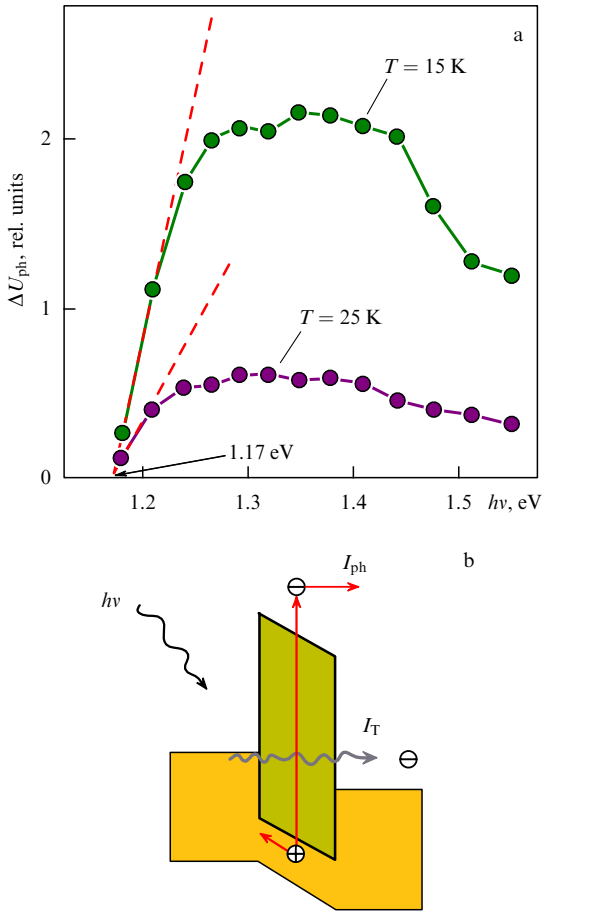

Figure 20. The $LSMO/LSM_{1-\delta}O/MnSi/SiO_2$ structure in the CIP geometry. (a) Spectral dependences of photoinduced changes ΔU_{ph} for $T = 15$ and 25 K. (b) Schematic diagram of a tunnel junction; along with the tunnel current I_T, optical radiation induces a photocurrent I_{ph} caused by the generation of electron–hole pairs during interband absorption in the insulating layer.

the potential barrier φ_0 of the tunnel structure under study is much lower than 1 eV and should strongly change at low temperatures due to a shift of the chemical potential in the MnSi layer after its transition to the ferromagnetic state. The barrier height changes from $\varphi_0 \cong 0.46$ eV at $T = 30$ K to $\varphi_0 \cong 0.79$ eV at $T = 5$ K. Thus, in the case of the photoemission mechanism, the value of $(h\nu)_{\rm th}$ should quite strongly change with changing the temperature, which was not observed in experiments. In addition, the barrier height should change upon changing the voltage across the tunnel junction because, due to the influence of specular reflection forces, a change in the voltage causes a change in the potential barrier height [7], but the value of $(h\nu)_{\rm th}$ remains invariable for any bias current (and therefore for any voltage across the junction).

Thus, the interband absorption of light with the formation of an electron–hole pair in the dielectric layer provides an additional contribution (apart from the tunnel contribution) from optically generated carriers to the total current through the junction. The photoresponse from the structure in the CIP geometry is not directly related to the generation of a photopotential at the tunnel junction, as could be expected for a single tunnel junction in the standard CPP geometry. The light causes an increase in the current through tunnel junctions, thereby controlling the current redistribution between the upper and lower layers of the structure. Due to the action of light, in both the absence and the presence of a magnetic field, the switching from the upper, low-conduction layer to the lower, high-conduction layer occurs already at small bias currents I. Correspondingly, the CVC branch after such switching runs much lower (corresponding to smaller V) than when optical radiation is absent. This change is clearly manifested in the CVC for $P > 30$ mW cm^{-2}, where photoinduced changes are saturated, i.e., the system in the stationary state.

Because the magnetoresistance effect is determined in our case by the resistance of tunnel junctions separating the layers of the structure and by its dependence on the magnetic field, while the photoinduced current through the junction in fact 'shunts' this resistance, the magnetoresistive effect should obviously decrease under irradiation, which was observed experimentally.

The complicated character of the CVC for optical radiation powers $P < 30$ mW cm^{-2} can be explained by specific features of the generation and relaxation of electron–hole pairs in the system in a strongly thermodynamically nonequilibrium state. The characteristic relaxation processes of photoexcited carriers occur in the insulating layer itself and in LSMO and MnSi layers having different properties. The situation is further complicated by the fact that the current flowing through the structure in the planar geometry that we use is determined by two asymmetric tunnel junctions connected in series such that their biases have opposite polarities.

Of course, the mechanism of the photoelectric effect in the example considered above does not differ from the mechanism observed earlier for classical nonmagnetic tunnel structures. Nevertheless, optical irradiation plays the role of an additional channel for controlling the transport and, indirectly, the magnetotransport properties of a magnetic tunnel junction. Conceptually, the discovered photoelectric effect can be promising for the development of radiation-controlled spintronic devices.

7. Conclusions

In this review, we have hopefully managed, to some extent, to put forward the fundamental problems of spin-polarized electron transport in manganite tunnel structures and to present the main results of experimental studies of spin-dependent phenomena in manganite-based structures. The applications of manganites attract interest because they have a number of unique properties such as a high spin polarization reaching 100%; a high Curie temperature; well-developed manufacturing technology; high chemical stability, and stability to external perturbations. All these make manganites promising materials for practical applications in elements of spintronic devices.

At present, we still cannot talk about wide applications of manganite-based magnetic tunnel structures for the reasons discussed in the review. At the same time, manganite-based tunnel structures have been extensively investigated because of their unique properties, and this allows us to talk in some sense about the limited but efficient practical application of these materials. Manganite-based structures reveal all the numerous effects observed in magnetic tunnel structures. They can be used to search for new manifestations of spin-polarized transport in nanostructures and for the development of new unique methods for studying spin-dependent effects in different classes of nanosystems.

We have demonstrated the observation of new manifestations of spin-polarized transport by new methods with the example of investigations of magnetic tunnel structures in the CIP geometry. This geometry is typically not used in tunnel structures. We have shown that the specific features of transport properties in planar geometry are related to the switching of current channels between conducting layers of the structure. The basic controlling elements here are the magnetic tunnel junctions separating the layers. The resistance of the junctions can in turn be controlled by the bias current, magnetic field, and electromagnetic radiation.

In this review, we have devoted much attention to the problems of spin-dependent electron transport in cooperative magnetic systems of magnetic tunnel junctions, which are quite attractive in fundamental and applied aspects. Manganites again prove to be unrivaled when dealing with efficient technologies for manufacturing such systems with predetermined characteristics.

Another field of investigation, which was not adequately described in the literature and which we briefly considered here, is the study of spin-polarized transport in magnetic tunnel structures in the case of combined external actions (transport current, magnetic and electric fields, microwave and optical radiation). These studies give additional information (compared to traditional methods) on the mechanisms of phenomena observed in tunnel structures and also allow finding new, efficient methods for controlling the spin-polarized current and the spin dynamics in these structures.

Finally, we hope that this review has convincingly demonstrated that the prospects of applications of manganite-based magnetic tunnel structures are far from being exhausted, and these structures will make a considerable contribution to the solution of the fundamental and practical problems of spintronics.

Acknowledgments. This work was supported by the Russian Foundation for Basic Research (grant No. 11-02-00367-a); the program of the Presidium of the RAS, Fundamental

Research on Nanotechnologies and Nanomaterials (grant No. 21.1); the program of the Department of Physical Sciences of the RAS "Spin Phenomena in Solid Nanostructures and Spintronics" (grant No. 2.4.4.1); integration projects of the Siberian Branch, RAS, Nos 5 and 134; and the Federal Special Purpose Program "Scientific and Pedagogical Personnel of Innovative Russia" (state contract No. NK-556P_15).

References

1. Fert A *Rev. Mod. Phys.* **80** 1517 (2008); *Usp. Fiz. Nauk* **178** 1336 (2008)
2. Grünberg P A *Rev. Mod. Phys.* **80** 1531 (2008); *Usp. Fiz. Nauk* **178** 1349 (2008)
3. Ralph D C, Stiles M D *J. Magn. Magn. Mater.* **320** 1190 (2008)
4. Kiselev S I et al. *Nature* **425** 380 (2003)
5. Suzuki Y, Kubota H *J. Phys. Soc. Jpn.* **77** 031002 (2008)
6. Simmons J G *J. Appl. Phys.* **34** 238 (1963)
7. Simmons J G *J. Appl. Phys.* **34** 1793 (1963)
8. Simmons J G *J. Appl. Phys.* **34** 2581 (1963)
9. Bardeen J *Phys. Rev. Lett.* **6** 57 (1963)
10. Stratton R *J. Phys. Chem. Solids* **23** 1177 (1962)
11. Harrison W A *Phys. Rev.* **123** 85 (1961)
12. Julliere M *Phys. Lett. A* **54** 225 (1975)
13. Chatterji T (Ed.) *Colossal Magnetoresistive Manganites* (Dordrecht: Kluwer Acad. Publ., 2004)
14. Volkov N et al. *Phys. Rev. B* **73** 104401 (2006)
15. Yuzhelevski Y et al. *Phys. Rev. B* **64** 224428 (2001)
16. Mercone S et al. *Phys. Rev. B* **65** 214428 (2002)
17. Raquet B et al. *Phys. Rev. Lett.* **84** 4485 (2000)
18. Zhao Y et al. *Phys. Rev. Lett.* **81** 1310 (1998)
19. Park S H et al. *Phys. Rev. B* **56** 67 (1997)
20. Nagaev E L *Usp. Fiz. Nauk* **166** 833 (1996) [*Phys. Usp.* **39** 781 (1996)]
21. Salamon M B, Jaime M *Rev. Mod. Phys.* **73** 583 (2001)
22. Dagotto E, Hotta T, Moreo A *Phys. Rep.* **344** 153 (2001)
23. Dagotto E (Ed.) *Nanoscale Phase Separation and Colossal Magnetoresistance*: *The Physics of Manganites and Related Compounds* (Springer Ser. in Solid-State Sciences, Vol. 136) (Berlin: Springer, 2003)
24. Pickett W E, Singh D J *Phys. Rev. B* **53** 1146 (1996)
25. Moodera J S, Meservey R H "Spin-polarized tunneling", in *Magnetoelectronics* (Ed. M Johnson) (Amsterdam: Elsevier, 2004)
26. Worledge D C, Geballe T H *Phys. Rev. B* **62** 447 (2000)
27. Park J-H et al. *Nature* **392** 794 (1998)
28. Lu Y et al. *Phys. Rev. B* **54** R8357 (1996)
29. Li X W et al. *J. Appl. Phys.* **81** 5509 (1997)
30. Viret M et al. *Europhys. Lett.* **39** 545 (1997)
31. De Teresa J M et al. *J. Magn. Magn. Mater.* **211** 160 (2000)
32. LeClair P et al. *Phys. Rev. Lett.* **86** 1066 (2001)
33. Moon-Ho J et al. *Phys. Rev. B* **61** R14905 (2000)
34. Bowen M et al. *Appl. Phys. Lett.* **82** 233 (2003)
35. Tsymbal E Y, Mryasov O N, LeClair P R *J. Phys. Condens. Matter* **15** R109 (2003)
36. Bowen M et al. *Phys. Rev. Lett.* **95** 137203 (2005)
37. Ghosh K et al. *Appl. Phys. Lett.* **73** 689 (1998)
38. De Teresa J M et al. *Phys. Rev. Lett.* **82** 4288 (1999)
39. Mitra C et al. *Phys. Rev. Lett.* **90** 017202 (2003)
40. Hueso L E et al. *Nature* **445** 410 (2007)
41. Schmidt G et al. *Phys. Rev. B* **62** R4790 (2000)
42. Rashba E I *Phys. Rev. B* **62** R16267 (2000)
43. Fert A, Jaffrès H *Phys. Rev. B* **64** 184420 (2001)
44. Dash S P et al. *Nature* **462** 491 (2009)
45. Naber W J M, Faez S, van der Wiel W G *J. Phys. D Appl. Phys.* **40** R205 (2007)
46. Dai J et al. *J. Phys. D Appl. Phys.* **33** L65 (2000)
47. Witanachchi S et al. *Appl. Phys. Lett.* **90** 052102 (2007)
48. Volkov N V et al. *J. Phys. D Appl. Phys.* **42** 065005 (2009)
49. Volkov N V et al. *Pis'ma Zh. Tekh. Fiz.* **35** (21) 33 (2009) [*Tech. Phys. Lett.* **35** 990 (2009)]
50. Volkov N V et al. *Rare Metals* **28** 170 (2009)
51. Ctistis G et al. *Phys. Rev. B* **71** 035431 (2005)
52. Ishikawa Y et al. *Phys. Rev. B* **16** 4956 (1977)
53. Klein J et al. *Europhys. Lett.* **47** 371 (1999)
54. Furukawa N *J. Phys. Soc. Jpn.* **66** 2523 (1997)
55. Hortamani M et al. *Phys. Rev. B* **74** 205305 (2006)
56. Mitra C et al. *Phys. Rev. Lett.* **90** 017202 (2003)
57. Volkov N V et al., Patent of the Russian Federation, No. 2392697 (Byull. 17, 20.06.2010)
58. Benz S P, Burroughs C J *Appl. Phys. Lett.* **58** 2162 (1991)
59. Sheng P, Abeles B, Arie Y *Phys. Rev. Lett.* **31** 44 (1973)
60. Helman J S, Abeles B *Phys. Rev. Lett.* **37** 1429 (1976)
61. Volkov N V et al. *J. Phys. D Appl. Phys.* **41** 015004 (2008)
62. Dey P, Nath T K *Phys. Rev. B* **73** 214425 (2006)
63. Liu J-M et al. *Appl. Phys. Lett.* **76** 2286 (2000)
64. Gupta A et al. *Phys. Rev. B* **54** R15629 (1996)
65. Hwang H Y et al. *Phys. Rev. Lett.* **77** 2041 (1996)
66. Shaykhutdinov K A et al. *Fiz. Tverd. Tela* **51** 734 (2009) [*Phys. Solid State* **51** 778 (2009)]
67. Niebieskikwiat D et al. *J. Appl. Phys.* **93** 6305 (2003)
68. Lee S et al. *Phys. Rev. Lett.* **82** 4508 (1999)
69. Shaykhutdinov K A et al. *J. Phys. Conf. Ser.* **200** 052025 (2010)
70. Calderón M J, Brey L, Guinea F *Phys. Rev. B* **60** 6698 (1999)
71. Salafranca J, Calderón M J, Brey L *Phys. Rev. B* **77** 014441 (2008)
72. Gupta S et al. *Appl. Phys. Lett.* **78** 362 (2001)
73. Balcells L et al. *Appl. Phys. Lett.* **74** 4014 (1999)
74. Petrov D K et al. *Appl. Phys. Lett.* **75** 995 (1999)
75. Taran S et al. *J. Appl. Phys.* **99** 073703 (2006)
76. Xia Z C et al. *J. Phys. D Appl. Phys.* **36** 217 (2003)
77. Chen T Y et al. *Phys. Rev. Lett.* **96** 207203 (2006)
78. Faris S M, Gustafson T K *Appl. Phys. Lett.* **25** 544 (1974)
79. Faris S M, Fan B, Gustafson T K *Appl. Phys. Lett.* **27** 629 (1975)
80. Miskovsky N M et al. *Appl. Phys. Lett.* **35** 560 (1979)
81. Van der Heijden R W et al. *Appl. Phys. Lett.* **37** 245 (1980)
82. Hartman T E *J. Appl. Phys.* **33** 3427 (1962)
83. Tulapurkar A A et al. *Nature* **438** 339 (2005)
84. Fan X et al. *Appl. Phys. Lett.* **95** 122501 (2009)
85. Volkov N V et al. *J. Phys. D Appl. Phys.* **41** 015004 (2008)
86. Volkov N V et al. *J. Magn. Magn. Mater.* **323** 1001 (2011)
87. Volkov N V et al., Patent of the Russian Federation, No. 2347296 (Byull. 05, 20.02.2009)
88. Fowler R H *Phys. Rev.* **38** 45 (1931)
89. Kadlec J *Phys. Rep.* **26** 69 (1976)
90. Kadlec J, Gundlach K H *Phys. Status Solidi A* **37** 11 (1976)
91. Kadlec J, Gundlach K H *J. Appl. Phys.* **47** 672 (1976)
92. Volkov N V et al. *J. Phys. D Appl. Phys.* **42** 205009 (2009)
93. Dagotto E, Hotta T, Moreo A *Phys. Rep.* **344** 1 (2001)